# soLi∂: Search for very short baseline Oscillation with a novel solid Lithium-6 detector

A. Baird[1], G. Barber[2], A. S. Cucoanes[3], M. Fallot[3], L. Giot[3], J. Nash[2], A. Rose[2], N. Ryder[1], P. R. Scovell[1], A. Vacheret[1], A. Weber[1], and F. Yermia[3]

[1]Department of Physics, University of Oxford, Keble Road, Oxford OX1 3RH, UK
[2]High Energy Physics Group, Blackett Laboratory, Imperial College London, UK
[3]SubaTech, UMR 6457, 4 Rue Alfred Kastler, La chantrerie, Nantes, France.
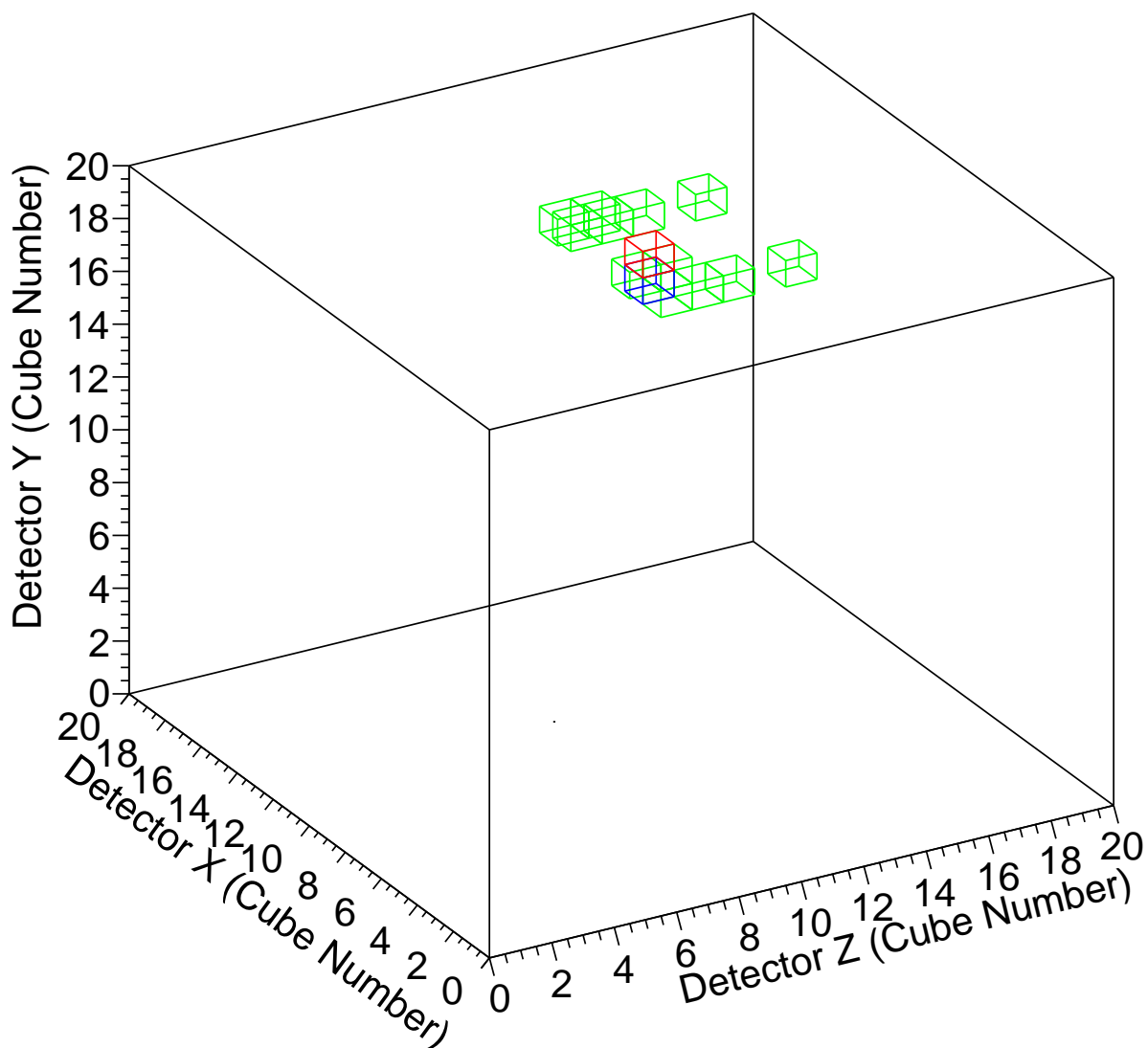
1 Executive Summary

The last decades have seen some major breakthroughs in the field of neutrino physics with the discovery of oscillations and, a year ago, with the last mixing angle θ_{13}. This proposal aims to address the anomalies currently persisting in the electron neutrino sector which could be an indication of the existence of a fourth neutrino in the form of a heavier sterile state. The possible existence of sterile neutrinos is not excluded by models and other observations and could have been missed by previous experiments at research reactors. Because neutrinos are the most abundant massive particles in the universe they play a major role in its evolution. The discovery of an additional neutrino would have some large consequences not only to the standard model of particle physics, but also to the understanding of the early dynamic of the Universe. New direct measurements at close stand off to compact nuclear reactor cores are therefore necessary to solve these anomalies and to give a definitive answer to this question.

The project proposed here uses a novel composite scintillator technology to detect antineutrinos with unprecedented sensitivity and to discriminate against backgrounds in a way unreachable with current state-of-the-art detectors. It addresses the key challenges necessary to:

- Allow the successful construction and deployment of one of the module of a new type of antineutrino detector at short distance from the reactor of the Institute Laue Langevin (ILL) in Grenoble, France followed by a run at the BR2 research reactor in Mol, Belgium; including a phase of integration and commissioning at the relevant institutes and on site at the ILL.

- Support the comprehensive development of a new approach to detector triggering using forefront FPGA-based digital pulse processing as well as the provision of custom made digitiser electronics.

- Allow he development of the Data acquisition system and interface for online data taking and monitoring.

- Undertake the testing campaign to calibrate accurately the detector neutron and positron efficiency using a beam of well-known neutron fluence and various sources like AmBe to demonstrate time coincidence measurement.

- Develop new reconstruction algorithms to select antineutrino interactions with high signal to noise ratio as well as the analysis to determine the sensitivity to oscillation by fitting the data both in energy and length, incorporating to information from calibrated and reconstructed quantities.

This proposal represents a unique opportunity to establish fully this new path of research and develop the expertise for future projects. The results promised in this proposal are far reaching both in science and in the development of future technologies for neutron and antineutrino detection.

2 Introduction

Neutrinos are by far the most abundant massive particle in the Universe. They, however, only interact weakly with matter and are therefore difficult to study. It took a few decades and a vast number of experimental results to establish that neutrinos oscillate from one type to another giving indirect evidence that neutrinos have mass, the first evidence of new physics beyond the standard model of Particle Physics. Indeed, the oscillation is a consequence of quantum mechanical mixing of the neutrino mass and weak flavour eigenstates, governed by the Pontecorvo-Maki-Nakagawa-Sakata matrix. For three neutrino flavours (electron, muon, tau) the oscillation is driven by three mixing angles ($\theta_{12} \approx 34°$, $\theta_{23} \approx 39°$, θ_{13}), a CP violation phase (Δ_{CP}) and by two independent mass-squared differences: $\left|\Delta m_{32}^2\right| = |m_3 - m_2|$ the so-called atmospheric mass splitting and $\Delta m_{12}^2 = m_2^2 - m_1^2$ the solar splitting. A year ago the third mixing angle θ_{13} was discovered and precisely measured ($\theta_{13} \approx 9°$) at nuclear reactors by the Daya Bay [4], RENO [5] and Double-CHOOZ [3] experiments after first indications given by the accelerator experiments T2K [1] and MINOS [2]. The sign of Δm_{32}^2, which determines the mass hierarchy, is still unknown and together with Δ_{CP} are now the focus of an intense new experimental programs. The standard three neutrino flavour mixing framework is well established and supported by a large amount of data from solar, atmospheric and accelerator data.

Not all results, however, fit with the current three neutrino picture: a few anomalies for very short baseline oscillation measurements have emerged. The first hint come from the GALLEX [6] and SAGE [7] experiments which measures the rate of neutrinos coming from the sun in the 1980s and 1990s. Both detectors consist of large volume of liquid Gallium with a diameter of 1.9(0.7) m for GALLEX(SAGE). The detection efficiency was calibrated using intense 51Cr and 37Ar radioactive sources placed inside the detector active volumes. ^{51}Cr and ^{37}Ar sources emit electron neutrinos via inverse beta decay (IBD) and can be detected using the same reaction used for the detection of solar neutrinos :

$$\nu_e + {}^{71}Ga \rightarrow {}^{71}Ge + e^- \; (E_\nu > 0.233 \; MeV). \tag{1}$$
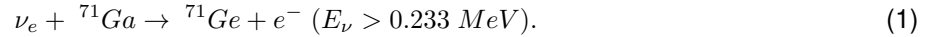
The number of neutrino events in the tank can be estimated from the cross-section calculation for each ν_e line emitted by ^{51}Cr and ^{37}Ar . The results of these calibration runs gave an average ratio of $R^{\text{Ga}} = 0.86 \pm 0.05$ which is about 2.8σ from the predicted value and is referred to as the Gallium anomaly [8].

The second hint is more recent and arose from a more precise evaluation of the anti-neutrino flux by collaborators of the Double-CHOOZ experiment [9] to help achieving a more precise measurement of the mixing angle θ_{13}. This type of experiment uses large detectors placed at 1 km baseline from a nuclear reactor. Nuclear reactors are very powerful sources of anti-neutrinos, which are produced along the chain of beta (β^-) decay of neutron-rich fission products. Power reactors emit around $2 \times 10^{20} \; \bar{\nu}_e/s/GW$ anti-neutrinos, which are detected via the IBD reaction in large liquid scintillator detectors doped with Gadolinium:

$$\nu_e + p \rightarrow n + e^+ \; (E_\nu > 1.805 \; MeV). \tag{2}$$
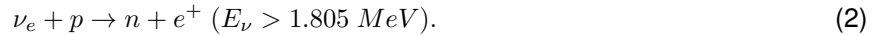
The threshold is given by the mass excess in the final state corresponding to $m_n - m_p + m_e$ where m_n is the mass of the neutron, m_p the mass of the proton and m_e the mass of the electron.

The measurement of neutrino oscillations at reactors is based on the observation of disappearance from one neutrino flavour to another, in this case the transition from an electron anti-neutrino to any other neutrino flavour. Since the detector is only sensitive to one type of neutrino, a deficit of events as a function of neutrino energy is observed. Similar to the SAGE and GALLEX experiments, the observed rate of interactions is compared to a predicted rate assuming no oscillation, which derives from theoretical calculations. Unlike recent experiments designed to search for θ_{13} using a relative difference based on a two-detector approach (one close to measure the un-oscillated flux and one far to measure the oscillated one), previous experiments searching for oscillations at baselines under 100 m had only one detector. These experiments therefore relied on a precise understanding of the anti-neutrino flux and cross-section calculation. Until about two years ago the data from reactor experiments agreed with the picture of oscillation between three neutrinos. The re-evaluation of the anti-neutrino flux from fission isotopes of ^{235}U, ^{238}U, ^{239}Pu and ^{241}Pu resulted in an upward shift in the prediction of about 3% [10]. This effect has been independently confirmed in another calculation [11]. The effect of this shift, combined with off-equilibrium effect and updated neutron lifetime measurements has a statistical significance of 2.9σ in the ratio of measured-to-predicted anti-neutrino events (total effect is (7.2 ± 0.5)%). This deficit is called the reactor anomaly. The consequence of this is that all previous experiments measuring the anti-neutrino flux see a deficit. Figure 1 from [12] shows the allowed region in the $\sin^2(2\theta_s) - \Delta m_s^2$ plane for the combination of reactor neutrino experiments, The GALLEX and SAGE calibration source experiments as well as the ILL and Bugey-3 energy spectra in the assumption of a 3+1 neutrino hypothesis. It can be seen that when combined, both anomalies disfavoured the no-oscillation hypothesis at 99.97% (3.6σ).

The most popular explanation for these anomalies is a new light neutrino which oscillates with other neutrinos at short distances. This additional neutrino cannot, however, interact weakly like the other active neutrinos
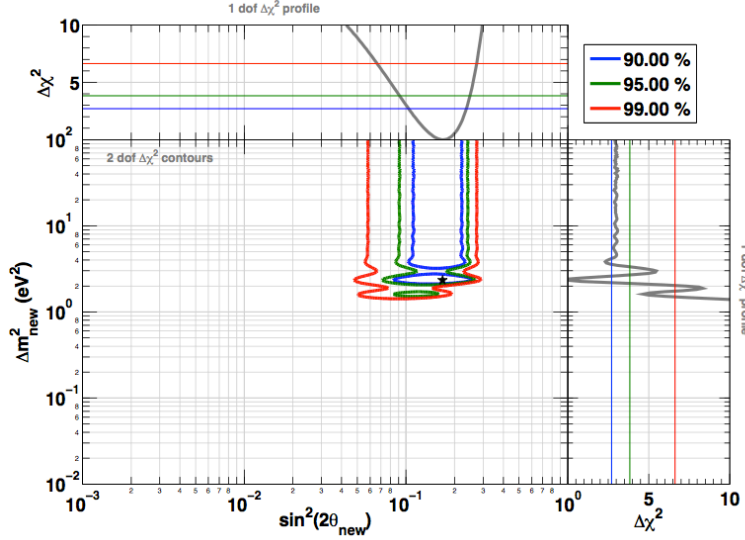
Figure 1: allowed region in the $\sin^2(2\theta_s) - \Delta m_s^2$ plane assuming a 3 active + 1 sterile neutrino hypothesis. The data combined all reactor experiments rate with ILL and Bugey-3 spectral information, as well as the GALLEX and SAGE source calibration data. The best fit point is at $\Delta m_s^2 = 2.3 \pm 0.1\ eV^2$.

since only three neutrinos have been found to couple to the Z boson in the LEP collider missing mass measurements at CERN. The only viable state for this new neutrino is to be "sterile" meaning that it doesn't interact through the weak interaction like the others. In the standard model this takes the form of a singlet state, while other neutrinos are part of a weak isospin doublet.

Sterile neutrinos appear naturally in many extension to the standard model but they give no constraint on what mass it should have. The theory only tell us that sterile neutrinos could be part of the physics beyond the standard model without indicating how they would mix with other neutrinos. This situation calls for new and better experimental data which is the only way to answer this question.

The neutrino community has taken these recent anomalies with concern and a white paper [12] has been written in 2012 to summarise the theoretical and experimental effort on the subject of light sterile neutrinos.

We propose to improve the search for oscillation at very short distance from a research reactor as the most direct and timely way to prove or reject the existence of sterile neutrinos. This new measurement will use an improved experimental setup, which has unprecedented sensitivity to new oscillation. In the case of a positive outcome, the community will be faced with the most extraordinary discovery beyond the standard model. Indeed, sterile neutrinos represent a very different type of new physics not investigated in mainstream high-energy experiments and would have far reaching consequences across disciplines.

On the other hand, an improved upper limit on their existence using reactor data will seriously weaken - if not rule out - the light sterile neutrino hypothesis as an explanation for these anomalies. Furthermore this new experiment will, independently of the outcome, help with improving the accuracy of the reactor anti-neutrino flux calculation, an important input for future experiments using reactors as anti-neutrino sources.

3 The soLi∂ experiment

The aim of the soLi∂ experiment is to search for disappearance of electron anti-neutrinos by measuring the anti-neutrino rate and energy spectrum using two 1.44 tonne detectors of a novel type at different distances. The detection reaction used is the well known Inverse Beta Decay reaction (equation 2).

Both detectors system will be standing between 6 and 10 m away from a compact nuclear reactor core to search for short distance oscillations and test the reactor anomaly. Figure 2 illustrates the experimental set up showing the two detectors (both split in five sub-modules) in front of the reactor wall at one of the possible site at the ILL (ILL-H7).

The energy distribution of anti-neutrino interactions measured in each sub-modules will be compared to identify energy and distance variations due to oscillations with minimal dependence upon the knowledge of the anti-neutrino flux. The maximum of oscillation for a $\Delta m^2 \sim 1\ eV^2$ is only about a few meters and to maximise the physics reach, a number of parameters needs to be taken into account:
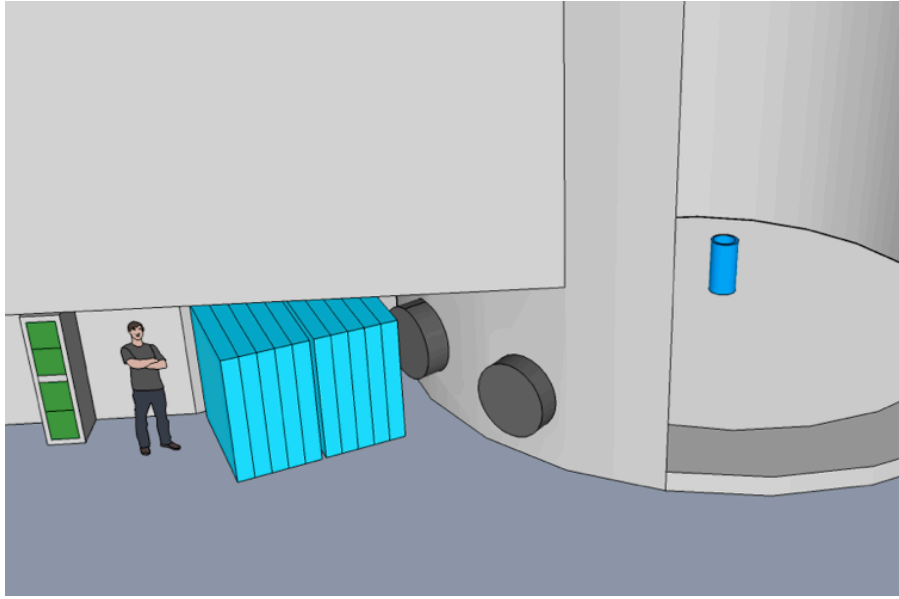
4

Figure 2: Schematic view of the SOLi∂ experimental set up at the ILL HFR reactor. The reactor core is on the right and the detectors are standing behind the H7 port (light blue) under the service pool.

- **Reactor Parameters:** Nuclear reactors are a pure source of electron anti-neutrinos through the β^- decay of fission products. The flux of anti-neutrinos is proportional to the thermal power output of the reactor with little time (i.e. isotope) dependence for a research reactor using highly enriched uranium-235 (HEU). A high reactor thermal power combined with long exposure time give maximum statistical power. Due the research purpose of these reactors, reactor ON-times are between $20-70\%$ per year. For instance, the ILL operates at 58 MW maximum licensed power for 300 days/year, which gives some of the best figure of merit of European research reactors. Unlike power reactor fuel, which is based on low enrichment of uranium-235 ($\sim$6%) and contains other significant proportions of uranium and plutonium isotopes (contributing to the anti-neutrino spectrum rate and shape), research reactors usually use HEU. They provide therefore a much more stable anti-neutrino spectrum over time as almost no other U and Pu isotopes are produced. The second reactor parameter is the size of the core. Anti-neutrinos are emitted isotropically and the core finite dimensions increase the spread in oscillation length between the point of creation in the reactor and the point of detection. This source extension degrades the capability to resolve the observable oscillation at the detector. Research reactors with dimensions ≤ 1 m^3 provide the most compact sources available. On-axis positioning of the detector is also preferable to limit additional extension effect by the source.

- **Detector Requirements:** The reactor facility has inherent constraints on where the detector can be deployed due to space restrictions. Reactors are usually immersed in a water pool surrounded by high density concrete walls to contain radiation, which limits the stand off distance typically to $5-6$ m from the core. The distance is an important experimental parameter as it determines the overall rate of anti-neutrinos as well as the oscillation length that can be probed. The detector fiducial volume and mass determines the number of observed interactions per day as the number of anti-neutrino interactions scales proportionally with the number of protons in that volume. This can be tuned, within space constraints, by increasing the acceptance available at a fixed distance. To fully characterise the oscillation phenomenon an observation both in anti-neutrino energy and distance from the core is required. The oscillation has a sinusoidal behaviour as function of energy and the effect shifts with distance (L/E effect). Only the demonstration of oscillation both in energy and position can form the evidence for a new oscillation. Good position and energy resolution is therefore required to maximise the experimental sensitivity.

- **Backgrounds:** One drawback of measuring anti-neutrinos close to research reactors is the need for operating the detector at the surface under low overburden. The main backgrounds are of cosmic ray origin and of reactor origin. These background depends on the overall configuration of the reactor and are site dependent. They can be reduced by passive and active shielding as well as discrimination techniques. There are two categories of backgrounds which could be mis-identified as anti-neutrino interactions and they are related to neutron and gamma-ray interactions in the detector: (i) fast neutrons (1–100 MeV) are either produced by the reactor and punching through the reactor wall or are produced

5

by spallation from cosmic muons stopping in the vicinity of the detector. These fast neutrons first scatter off protons from hydrogen atoms giving a fast signal similar to the positron and thermalise rapidly. They are absorbed by the neutron sensitive layer of the detector and give a time correlated signal, which are of similar duration to an anti-neutrino interaction. This is the correlated background and can be mitigated mainly with passive shielding. Some discrimination techniques are also employed to deal with these neutrons based on pulse shape discrimination. (ii) the second type of background is the accidental background: Large fluxes of gamma-rays are produced in the wall of the reactor from activation by neutrons, some of which have high energy (1-10 MeV). For large flux of gamma-rays and neutrons the probability to detect a gamma-ray and a unrelated neutron in a short time window become significant and could rapidly dominate the overall rate. Large walls of lead are usually used to significantly decrease the rate of gamma-rays by a few orders of magnitude. This in turns tends to increase the rate of neutrons which can enter the detector. The signal-to-noise ratio (S/B) gives a measure of the total fraction of background falling in the signal category. This S/B needs to be kept as high as possible to maximise the sensitivity to a new oscillation. Its value is however difficult to predict accurately because it relies on a very good knowledge of the background - a notoriously difficult task for any neutrino experiment. The energy dependence and the position distribution of this background can rapidly decrease the sensitivity of the experiment.

The experiment is planned to take place close to the High Flux Reactor (HFR) at the Institute Laue Langevin (ILL). A very similar configuration has also been studied at the BR2 reactor in Mol, Belgium. Both reactors have very similar core size and power.

The HFR reactor has a powerful 58 MW compact core (20 cm radius x 80 cm length) and the current baseline is to deploy the detectors at 6.5 m and 7.5 m away from the core just behind the concrete reactor wall. The reactor is pure ^{235}U and gives a very stable anti-neutrino spectrum over time. Precision flux calculations are based on the β-spectra of fissile isotopes performed at ILL in the 1980s[14] and a new high statistics measurement at the same type of reactor will improve our understanding of the flux calculation method.

3.1 Sensitivity to new oscillations

Neutrino oscillation is an energy dependent phenomenon and the only convincing way to test the sterile neutrino hypothesis is to measure a deficit of events as a function of anti-neutrino energy and distance. The anti-neutrino spectrum (un-oscillated) from IBD reaction is shown in Figure 3 on the left. The spectrum peaks at around 3.5 MeV and ranges from 1.8 MeV up to 15 MeV. Oscillations will distort the shape of this spectrum.

In a two flavour approximation the oscillation survival probability is

$$P_{ee}\left(E_{\bar{\nu}_e}, L, \Delta m_s^2, \theta_s\right) = 1 - \sin^2\left(2\theta_s\right)\sin^2\left(1.27\frac{\Delta m_s^2[eV^2]L[m]}{E_{\bar{\nu}_e}[MeV]}\right), \tag{3}$$

where θ_s is the mixing angle, which is determines the amplitude of oscillation between the two neutrino flavours, Δm_s^2 is the difference in squared masses, $E_{\bar{\nu}_e}$ is the anti-neutrino energy and L is the distance from creation to detection. The oscillation analysis is therefore based on the measurement of the anti-neutrino energy as a function of the distance. This effect is illustrated on the right of Figure 3 for the reactor anomaly best fit values $\Delta m_s^2 = 2.3 \pm 0.1 eV^2$ and $\sin^2(2\theta_s) = 0.17 \pm 0.04$. The analysis will use the fine segmentation of the detector to split the fiducial volume of the detector in an optimised set of distances. The minimal segmentation of the volume achievable is 5 cm. The distance shown on the right figure is set to 10 cm and illustrates the granularity achievable for resolving the oscillation pattern (i.e. the position of minima of oscillations varying with distance from the core).

Since the current anti-neutrino flux calculation may have unknown biases, the analysis will compare the shape of the spectrum accumulated at various distances and be largely independent of the flux.

The detection of anti-neutrino is bases on the IBD reaction (Equation 2) and an estimation of the expected rate of interactions per tonne of fiducial volume can be calculated using the knowledge of the IBD cross-section and a parametrisation of the anti-neutrino flux (see Equation 106 in [12]). The average number of anti-neutrino interactions at a distance of 7.5 m is $R_{\bar{\nu}_e} \approx 2130/\text{day}/2.88$t . The preliminary detection efficiency of 41% has been estimated using GEANT4 simulation (see Section 10.3). Assuming 300 days operation of the ILL per year and a total run period of two years, SOLi∂ will collect a total of 262k events.

The measure of the sensitivity to new oscillations is based on a shape only analysis, where the difference between distance bins is computed. These bins are slices of 20 cm corresponding to a detector sub-module along the core axis. More precisely the first distance bin (the sub-module closest to the reactor core) is taken as a reference for the anti-neutrino spectrum and is compared with the other distance bins. Using this approach, one can consider only uncertainties related to the variation of the detector properties along the distance axis. In this case two main systematics are considered:
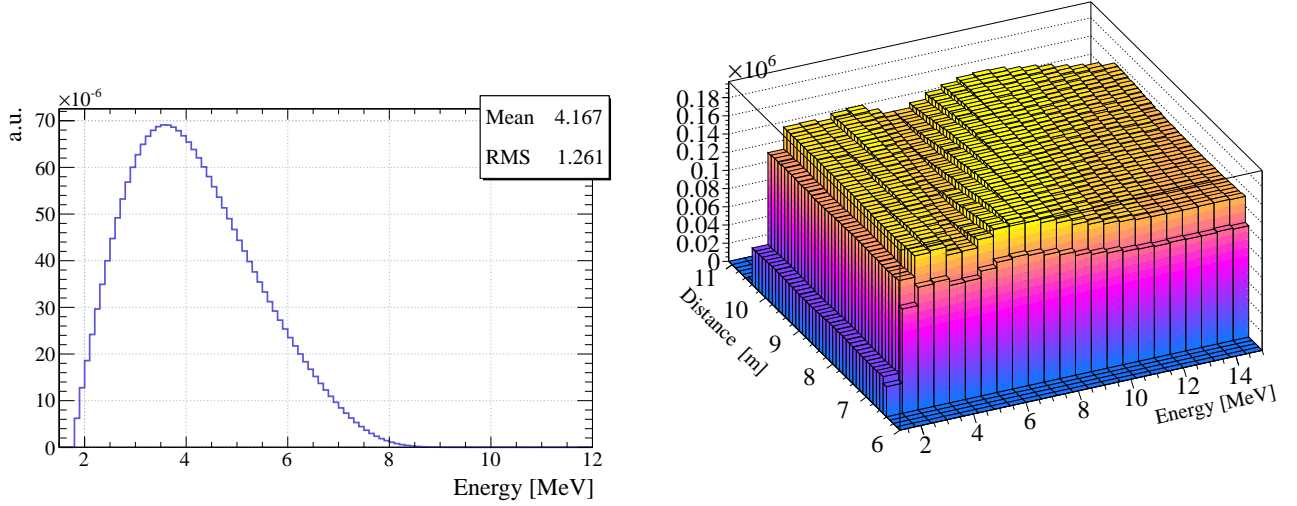
Figure 3: (left) Energy spectrum of the ILL reactor anti-neutrinos interacting in the sOLi∂ detectors. (right) Effect of oscillation to a sterile state for the global best fit values $\Delta m_s^2 = 2.3 \pm 0.1 \ eV^2$ and $\sin^2(2\theta_s) = 0.17 \pm 0.04$ as a function of distance and energy. The binning in distance is 10 cm and 500 keV in energy.

- Bin-to-bin uncorrelated error related to the background subtraction. We consider this error as equal to the statistical error per bin of the background shape and we added it in quadrature to the total systematical error.

- Systematical error related to the variation of the detector properties along the distance axis (σ_n). This error is related in principal to the solid angle correction between different detector slices.

Using the ratio of spectra from various distance the significance of the measurement can be determined for any possible value of oscillation parameters with the following χ^2 function :

$$\chi^2 = \sum_{d>1} \left[\sum_i \left(\frac{R^{i,1}(1+\alpha_n^d) - R^{i,d}}{\sigma_m^{i,d}} \right)^2 + \left(\frac{\alpha_n^d}{\sigma_n} \right)^2 \right] \tag{4}$$

where

$$\sigma_m^{i,d} = \sqrt{R^{i,d} + B^{i,d} + R^{i,1} + B^{i,1}} \tag{5}$$

In these expressions we considered the measured anti-neutrino rate per energy bin i of the first (closest to reactor) detector slice as $R^{i,1}$, the rest of detector slices as $R^{i,d}$ and the background contribution $B^{i,d}$. The solid angle correction is already taken into account before subtraction. Distance parameter α_n^d is the associated systematic error σ_n and is used for the χ^2 minimization.

The contours at 5σ confidence level are shown in Figure 4 for the preferred site with $R^{i,1}$ measured at 6.5m from the core on level C in front of H7. The calculation includes a detector efficiency of 41%, a reconstructed energy threshold at 600 keV and energy bins of 500 keV.

3.2 The sOLi∂ detector system

The sOLi∂ detector is the product of detector technology development made through the MARS project [15]. This project started at Imperial College London and Oxford in the period 2009-2011 with the aim of developing novel types of neutron and anti-neutrino detectors for science and applications in security, dosimetry and the nuclear industry. The MARS technology is protected by a patent (PCT/GB2012/052097- composite scintillator detector) and the innovation of the system is drawn partly from recent development made for the STFC funded T2K experiment. The patent is been already exploited with the development of new radiation detectors with industrial partners. The high sensitivity achieved with MARS has been applied to the detection of anti-neutrinos. The development of a new antineutrino detector has been motivated by the need for a robust and highly sensitive yet practical monitoring system for reactor safeguards (more details can be found in the pathway to impact about this). The requirements for such detectors are very similar to the one that needs to perform a precise spectral measurement in a difficult environment close to a research reactor. The excellent
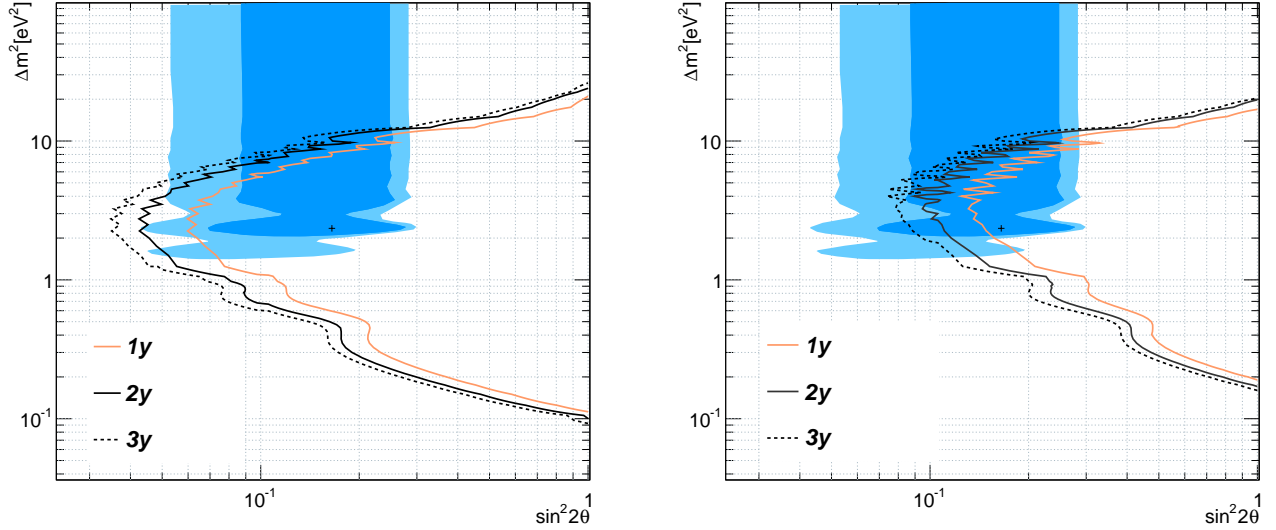
Figure 4: (left) Contours at 5σ with the two SOLi∂ detector configuration (2.88t) for 1,2 and three years running at 300 days/year. 99% light blue and 95 % navy blue allowed region of the global fit to the reactor and Gallium anomalies assuming a 3+1 neutrinos hypothesis. (right) same contours but for only one detector configuration at the closest distance.

performance reached in neutron efficiency and purity with the MARS neutron portal system gave us the confidence that a highly sensitive antineutrino detector can be build based on the same principles. In the following, we describe who the detector works, the expected performance for detecting anti-neutrinos and the strategy to reject background events.

3.2.1 Detection principle

The detector described here is a paradigm change compared to Gd doped Liquid Scintillator detectors. The volume providing the hydrogen target is made of Poly-Vinyl Toluene (PVT) segmented in cube of size of ($5 \times 5 \times 5$) cm covered with a layer sensitive to thermal neutrons. As shown in Figure 5 (left), an anti-neutrino interacts with a proton in one of the PVT cubes producing a positron and a neutron in one of the detector cubic element. The outgoing neutron thermalise and is eventually absorbed on the layer rich in ^{6}Li (^{6}LiF:ZnS(Ag)) between a few hundreds of nanoseconds to few hundreds of microseconds. Figure 5 (right) shows the difference between the "prompt" scintillation signal and the "delayed" one from the neutron. As the neutron average kinetic energy is around 10 keV it doesn't always get absorbed in the same cube as the positron which opens the possibility of directional measurement.

The mixture of ^{6}LiF:ZnS(Ag) is semi-transparent to its own light and works well in the form of a thin layers of a few hundred microns. This heterogeneous layer is made rigid with a binder and optically coupled to one side of the PVT cube. The reaction for the capture of the neutron by ^{6}Li is:

$$n +^6 \text{Li} \rightarrow^3 \text{H} + \alpha + 4.78 \text{ MeV}. \tag{6}$$

This reaction has a high cross-section for thermal neutrons (936 barns at 1.8 Å compared to 0.33 for Hydrogen). The outgoing nuclei have sufficient kinetic energy to escape a few tens of micron in the mixture and excite the surrounding grains of ZnS. ZnS is one of the brightest inorganic scintillators and has a very low quenching factor. A neutron converting in the layer produces 160 000 photons per neutron. Due to the large ionisation density created by the tritium and alpha particle, neutron signals have long decay constants (of the order of ten microseconds). The thin layers reduces sensitivity to gamma-rays and any interacting in the layer produce fast pulses only. A typical signal from a neutron in the ^{6}LiF:ZnS(Ag) is shown in Figure 6 along with a typical electromagnetic excitation signal from a gamma-ray. The signature from a neutron event is, therefore, very different from that of a gamma-ray, providing an effective discrimination between the two event types.

The discrimination between a neutron and other species gives the possibility of using the neutron as a reference for triggering the SOLi∂ detectors. Figure 7 shows the integrated charge over 2μs of a triggered event versus the total number of peaks counted in the tail of the waveform during that time in a single MARS

8
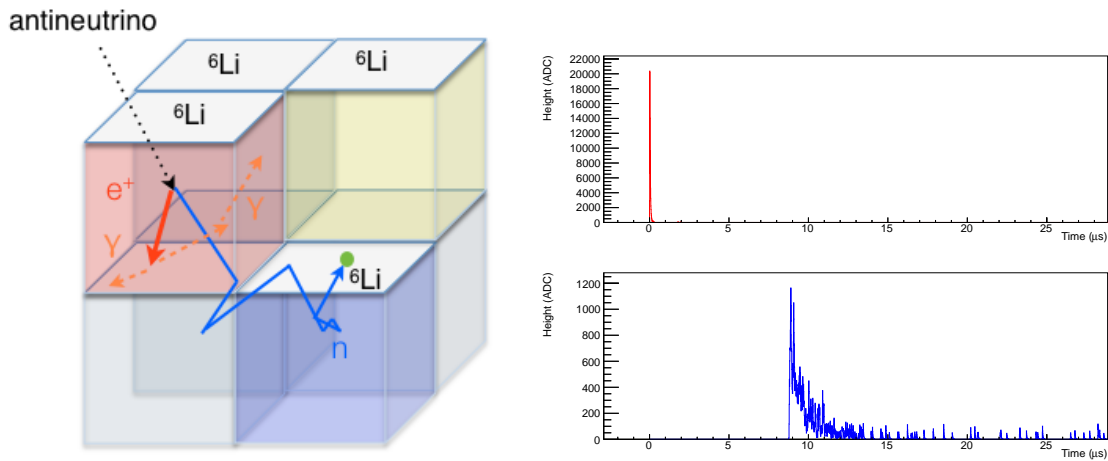
Figure 5: (left) Detection principle of MARS anti-neutrino detector. (right) Monte Carlo simulation of waveforms for the prompt positron signal (top) and delayed neutron event (bottom).
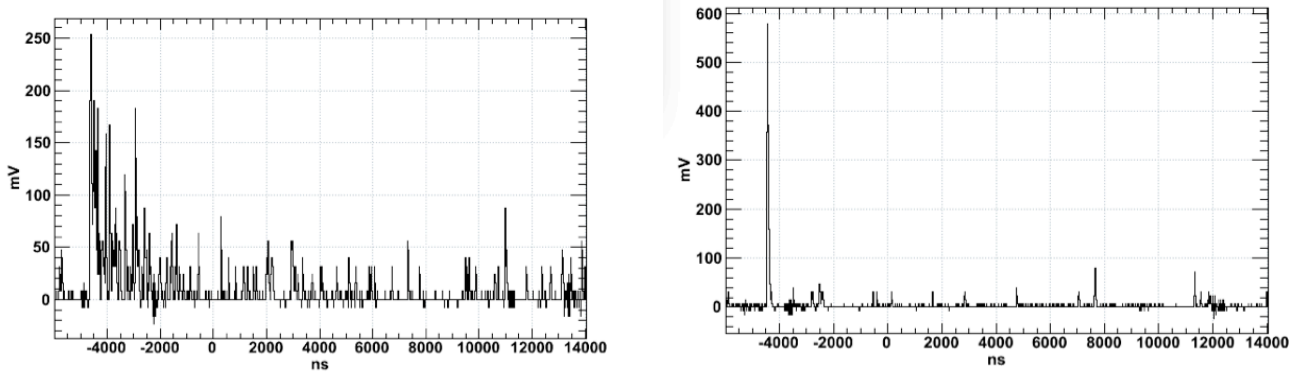
Figure 6: (left) waveform of the signal collected from a neutron capture in the ^{6}LiF:ZnS(Ag) layer. (right) waveform of a gamma-ray signal in the PVT.

cube exposed to an AmBe source. A discrimination power between 10^{-4} and 10^{-7} can be achieved with this technique.
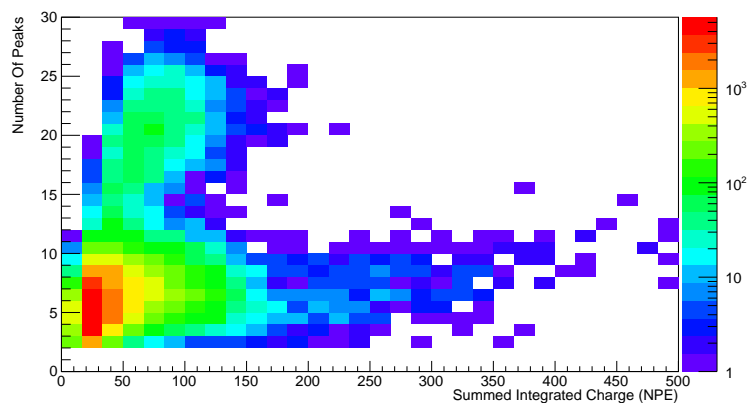
Figure 7: Integrated charge versus the number of peaks of trigger pulses registered in a MARS anti-neutrino cell exposed to an AmBe source.

3.2.2 Scintillation light read out

The scintillation photons produced by the positron in the organic scintillator and by the neutron in ^{6}LiF:ZnS(Ag) are collected and shifted to green light using large cross-section (3 mm x 3 mm) square wavelength shifting fibres (BCF-91A) running through grooves in all the cubes (shown in Figure 8 for a a stack of 64 cubes).
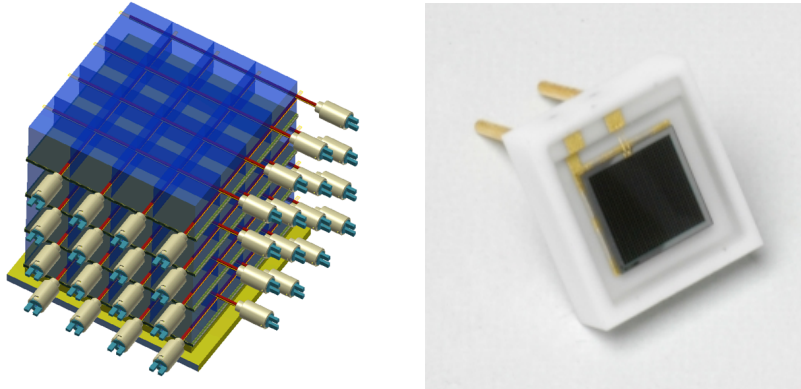
Figure 8: Schematic of a stack of cubes showing the WLS fibres read out configuration and connectors for the coupling with photosensors. Picture of a 3mm x 3mm MPPC in his ceramic package (right).

The green light is transmitted to the end of the fibre and collected by Geiger mode Avalanche photo-diode (also called SiPM). The SiPM candidate for the detector is the Hamamatsu Multi-Pixel Photon Counter (MPPC) 3mm x 3mm shown on the right of Figure 8. The network of fibres in this configuration ensures that any signal in any one cube can be detected accurately.

This novel approach offers some unique advantages :

1. The neutron scintillation signal is very specific and can be well discriminated against fasts electromagnetic signals.

2. Both prompt and delayed scintillation signal are read out through the same channel minimising the number of channels per tonne of fiducial mass.

3. Both neutron and positron are detected close to each other (within a few cm) providing very good localisation of the interaction. This limits the effect of background interference to a small volume around the interaction vertex.

4. The segmentation of the fiducial volume provides good spatial resolution for interactions and provides information about their topology. This can be exploited to recognise true anti-neutrino interactions and also to determine the source of background. Furthermore, this enables the possibility to divide the detector in various thicknesses of active volume increasing the sensitivity of the oscillation measurement.

5. the network of fibre and the long distance light attenuation provides good light yield uniformity and enable precise energy measurement.

3.2.3 Digitiser electronics and digital pulse processing

The electronics will fully exploit the features of the neutron signal. The detector will be read out by digitiser electronics with sampling resolution of 16 ns and a new approach using FPGA based Digital Pulse Processing (DPP) will be implemented to recognise neutron events based on the properties of the pulse (shape and width of signal, number of peaks in the tail etc). The neutron signal will then be used to trigger the system to limit the sensitivity to electromagnetic signal from gamma-rays and muons. The rate of neutrons is expected to be low (10–100Hz) and the full system will be read out at every neutron detected and recognised by the DPP algorithms. A window of 200–300 μs before the trigger will be kept in memory to look for the positron signal and reconstruct the coincidence signature of an anti-neutrino event. This new type of trigger will be tuned and optimised in the real system using the coincidence between de-excitation gamma-rays and neutrons from an AmBe source readily available in Oxford and Imperial College.

3.2.4 sоLi∂ detector modules

The sоLi∂ anti-neutrino detectors consist of 11520 scintillator cubes and have the following dimensions: 1.2 m width x 1.2 m height x 1 m depth. A schematic of one detector is shown in Figure 9. The total number of read out channels is 1920 (SiPM read out at both ends) and the overall footprint of the detector is expected to be roughly $(1.5 \times 1.5 \times 1.2)$ m. All sides of the detector have an additional polyethylene panel to reflect IBD neutrons escaping from the target volume. The MPPC read out and electronics are kept outside the fidicial volume for easy access and to limit inhomogeneities.
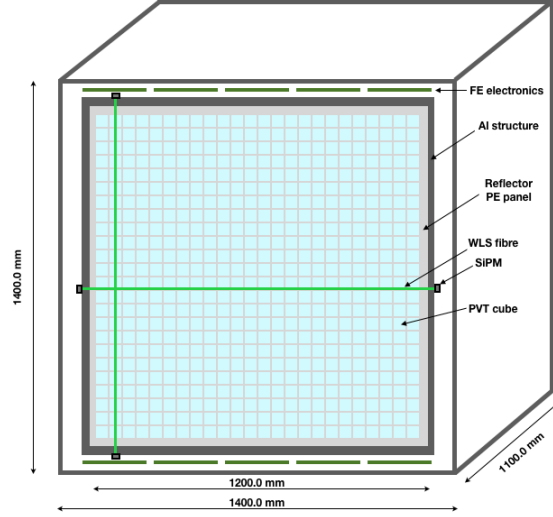

Figure 9: Schematic of the sоLi∂ detectors. The fibre orientation is shown for X and Y directions.

Some additional thickness of shielding against neutrons will be added around each detector module. A total 20 cm thickness of PE with 5 cm of Borated PE has been considered for the experiment. The gamma-ray shielding is expected to be limited to a position in front of the the reactor wall. The total weight on the ground is expected to be of a few tonne per m^2.

3.2.5 Light yield

The measurement of the positron energy is key to reconstruct the energy distribution of the anti-neutrino. Indeed the large mass difference in equation 7 means that we can consider all the kinematic, energy transferred to the lepton. With the high granularity of the detector, we can differentiate between the positron deposited energy and the one from the gamma-rays of its annihilation. The visible energy is therefore directly related to the anti-neutrino energy :

$$E_{vis} = E_{\bar{\nu}_e} - 1.804 \ MeV \tag{7}$$

For a precise energy measurement the positron has to deposit most of its energy in a single cube and be detected with high efficiency. The light yield was measured with cosmics and was found to be ~ 5 photoelectrons per MeV per fibre end. This value was measured at distance of 50 cm from the cube. An excellent energy threshold was determined to be around 50 keV. The simulated positron spectrum and integrated neutron spectrum are shown on Fig. 10. The corresponding energy resolution achievable is $\sigma E/E \approx 0.25$ at 1 MeV which is good enough to reach a high sensitivity to oscillation (see for example [13] for a complete study).

3.2.6 Anti-neutrino Detection efficiency

To determine the anti-neutrino efficiency a simulation of the sоLi∂ anti-neutrino detector was performed using a GEANT4 model with optical photon tracking enabled. This simulation is based on previous neutrino and dark matter experiments (T2K and ZEPLIN–III). Reconstruction of the IBD events was performed with a simple analysis code. The reconstruction of the IBD event was performed by first selecting a neutron event. The expected efficiency of detecting a neutron event was taking into account. To reconstruct the positron signal a spatial cut ($\delta x = 15 cm$) was defined around the position of the neutron (see figure 11).

In addition to this, a time cut was defined to demand that any positron signal must precede the neutron signal by between 300 ns and 200 μs. Finally to avoid picking up low energy gamma-rays, an energy cut of $E > 600 keV$ (~ 15 PE) was required. Table 1 summarises the steps of the analysis and the survival probably
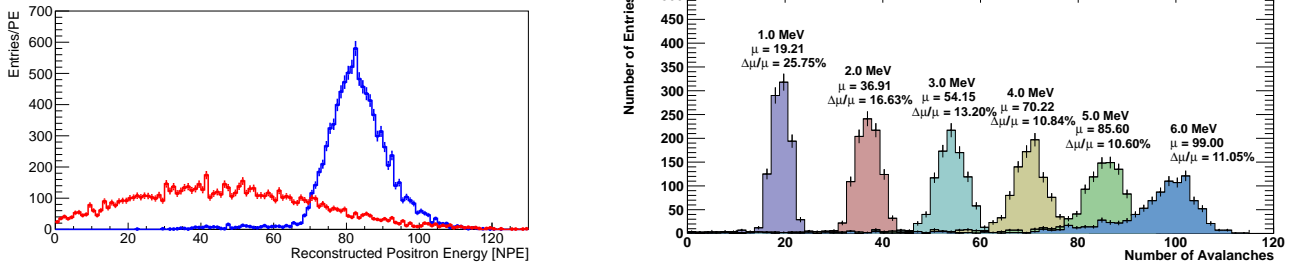
Figure 10: integrated signal of positron (red) and neutron (blue) waveforms (left). The neutron waveform signal is integrated over 20 μs. Monte Carlo generated response of the sOLi∂ detector to mono energetic positrons in the range of IBD energies (right).
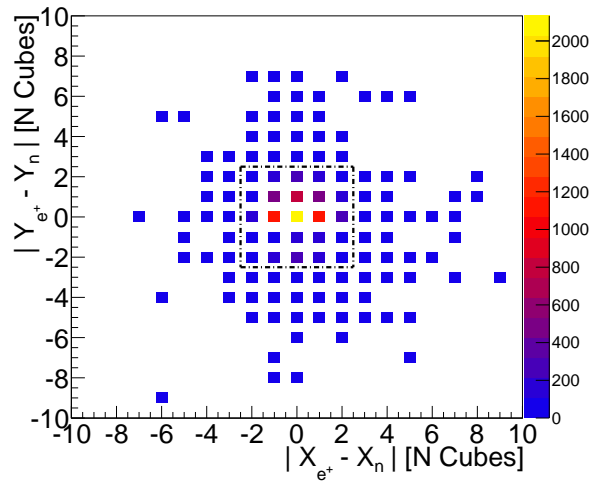
Figure 11: Cube distance between the neutron trigger and the positron signal. Most events have both signal well within 15 cm of each other.

based on 2000 generated events in the detector. The efficiency is mainly driven by the ability to detect the neutron. The detection efficiency being based on a different system that has a lower light yield, we expect the overall efficiency of the full scale system to be closer to 50%.

Table 1: Inverse Beta decay event selection cuts

Cut	Survival probability
neutron capture on ^{6}LiF:ZnS	0.64
neutron trigger	0.45
Energy threshold	0.44
δx and $E_{vis} >$600 keV	0.42
300 ns $< \delta t <$200 μs	0.41

The assessment of the reconstruction capabilities of the sOLi∂ detector is just starting and many handles can be found to reject background and identify the IBD event topology. The figure Fig. 11 also shows that the detector has some sensitivity to the direction of the anti-neutrino (flux generated in the +Y direction) increasing the possibility of selecting very pure samples of IBD events.

3.2.7 Sensitivity to Backgrounds

The sOLi∂ detector with its fine granularity and precise position resolution has unprecedented capability to reject background events. Preliminary studies have shown very promising rejection of the main backgrounds.

12

Fig. 12 shows the visible energy from fast neutrons and gamma-ray backgrounds.
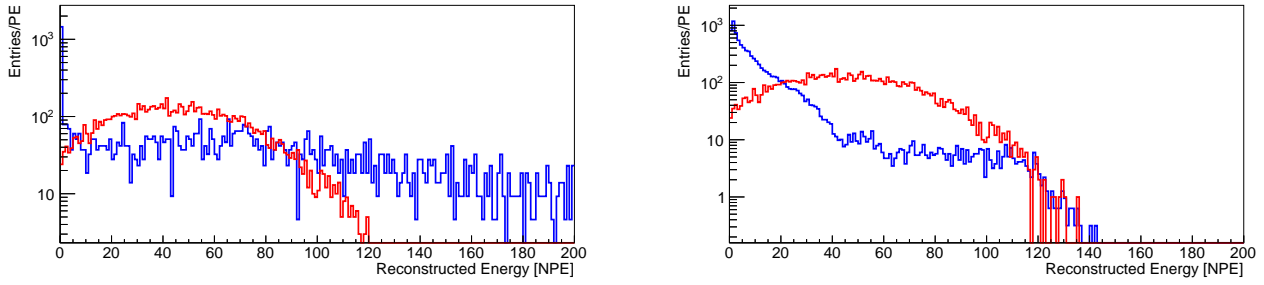
Figure 12: Visible energy of fast neutron events absorbed in the ^{6}Li layer (blue) on top of positron energy spectrum (red) normalised to the same number of events (left). Visible energy of gamma-rays from a spectrum measured at ILL on top of the same positron distribution (right).

The granularity of the detector already offers ways to reduce the level of background without requiring large amount of passive shielding. For fast neutrons, the good localisation of the neutron capture makes it difficult to survive the IBD time and position cuts. The effectiveness of such selection cut (reducing correlated events to around 5% of the pre-cut value above 20 PE) is shown on left Fig. 13. The topology of gamma interactions gives large number of hits and can be reduced by looking at low energy coincidences between cubes. This type of Compton cuts are out of reach to standard Liquid scintillator detectors due to their coarse segmentation. Left Fig. 13 demonstrates the effect of the cut on gamma-rays depleting most of the high energy part of the spectrum hence reducing by an order of magnitude the level of uncorrelated background. The cut reduces the background associated with gamma-ray events to ~7% of the uncut level above 20 PE.
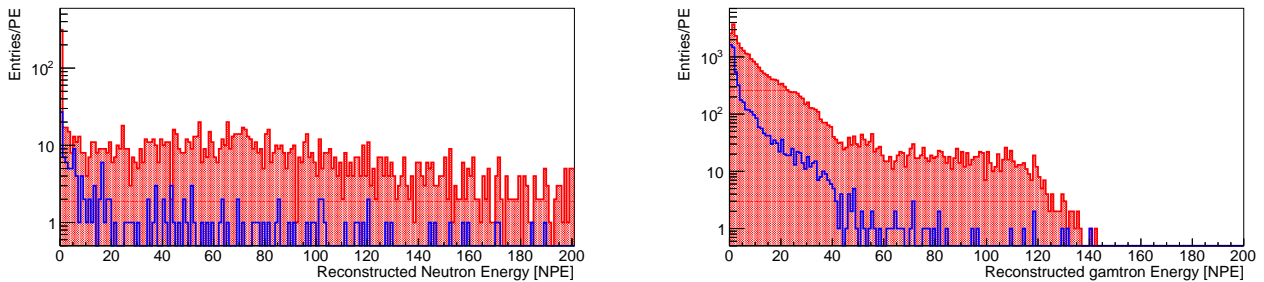
Figure 13: Visible energy of fast neutron events absorbed in the ^{6}Li layer (blue) before and after the IBD selection cuts (left). The cuts reduce the level of correlated background down to around 5% of the uncut events above 20 PE. Visible energy of γ-rays from a spectrum measured at ILL before and after the IBD + Compton γ-ray rejection cuts (right). The cuts reduce the expected rate of gamma-ray interactions above 20 PE to ~ 7% of the uncut value.

Table 2 summarises the rate of background events in the presence of a 10 m water equivalent overburden in addition to the detector shielding. The fast neutron rate and atmospheric neutron rate have been derived from measurement at ILL. The accidental rate is reduced dramatically with the temporal and spatial cuts used in the analysis. The exceptional granularity of the detector enables the precise study of the background and of its spatial distribution. A signal to background ratio of 3 can be achieved ensuring a minimum impact of the background to the measurement without the need for a large mass of passive shielding.

The granularity will also give the capability of a good rejection of the cosmic muons going through or stopping in the detector without the need for a external muon veto.

4 Competing research

A large number of projects have been proposed to search for oscillations at short distances. They can be split in three main categories : measurements at research and power reactors, deployment of very intense radioactive sources at existing large liquid scintillators and accelerator based experiment.

Table 2: Summary of detected signal and background by category

type	Ev/s/cm^2	H7 Ev/tonne/day 7 m	Ev/tonne/day (Shield+IBD cuts)
Anti-neutrino	6.94×10^{-7}	850	349
Reactor ON gamma-ray	1	1.21×10^9	24×10^6
Reactor ON fast neutrons	2.4×10^{-3}	2×10^6	26
Atmospheric neutrons	8×10^{-4}	6.9×10^5	43
Accidentals			3
Intrinsic radioactivity			12

- **Short baseline reactor experiments** (details in [12]): two experiments - Nucifer (OSIRIS, CEA, France) and DANSSino (Kalinin PWR, Russia) - are currently running with low mass prototypes. Nucifer started taking data in April 2013 and will run for a few months. DANSSino has already taken some data (April-October 2012) to validate the technology and data analysis is currently underway. Nucifer was delayed for two years due to safety regulations and a high level of background has prevented the detection of neutrinos thus far. These experiments are demonstrators and may see a hint of a new oscillation in their analysis but are not currently able to make precise measurements. Detectors based on liquid scintillator (LS) technology include STEREO at ILL (2t) and NEUTRINO-4 at WWR-M/SM3 Kaliningrad, both with data taking starting in early 2015. Due the difficulty of Nucifer to run at OSIRIS, Gd-loaded liquid scintillator proposals are facing a great challenge and very large amount of shielding will be required. Both proposals are serious competitor for SOLi∂ and NEUTRINO-4 has already some funding to start designing the experiment. DANSS uses plastic scintillator and Gd and will start in 2015 at Kalinin with a baseline at 10-12m away from the core. SCRAAM is a US effort from LLNL at San Onofre PWR reactor. Despite a stand off farther away this experiment may run as early as mid 2014 and could give some hint to new oscillations as well. Both experiments have less sensitivity due the the size of commercial reactor cores but will be able to probe the mass region below 1 eV^2. Some other proposals at US research reactors are under investigation but the timescale for these is not clear and none of these are yet funded.

- **Intense sources** (also in [12]): Ce-Land is a French proposal to make a measurement with a ^{144}Ce source (MCi) at KamLAND. Borexino proposes to use a ^{51}Cr source. The advantage of this is the detector is already available but the development and shipping of such large sources are difficult and subject to tight regulations. The measurement can be done quickly, especially with the high energy neutrinos from the Ce source but an R&D phase is necessary which could take at least three to five years. The CeLand R&D phase is funded at the level of 1.5M Euros and Borexino also has some funding available for this effort. Both detectors are, however, already in use : KamLAND-Zen is currently running and the Borexino Solar neutrino run will last for another two years at least. KATRIN, a beta decay experiment measuring the mass of neutrinos, will have sensitivity to the sterile neutrino hypothesis and will start data taking in 2015. They could give good constraints by 2017.

- **Accelerator based experiment**: in the ν_μ sector MINOS+, Liquid Argon MicroBooNE and the LANL LAr detectors (to replace the MiniBooNE detectors at FermiLab) will start within a few years. These experiments will take an additional few years to get to the level of sensitivity required but could add some complementary measurement to the electron neutrino sector searches.

  In summary, the most serious competing reactor experiments are expected to have started by the beginning of 2015 with other types of experiments to follow. This proposal is therefore based on a start at ILL during this key period.

5 Research Reactors availability

The timeliness of the experiment depends upon the availability of the research reactor. There are two research reactor candidates for this experiment: The HFR reactor at the Institut Laue Langevin in Grenoble, France and the BR2 Reactor in Mol, Belgium. Both reactors have very similar power and core size and are both well suited for a very short baseline experiment. Fig. 14 shows the most competitive sites for deployment available at ILL and BR2.

- **ILL-HFR**: The ILL neutron source is used intensively by many different users and experiments. Some constraint of space and schedule are therefore associated with the installation of a short baseline neutrino
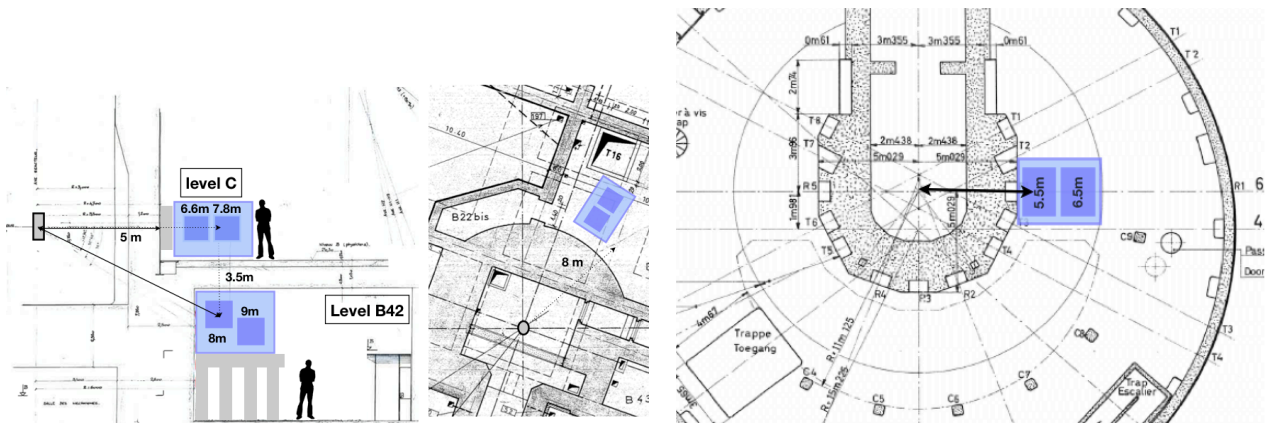
Figure 14: View of the area available on level C in front of ILL-HFR (cut view in vertical plane and level B) (left). Horizontal cut view of the BR2 reactor and area identified for the SOLi∂ experiment detectors at position R1 on the right hand side

experiment there. The ILL Science council has shown a very strong interest in hosting a very short baseline experiment for a period of two years with a possible start as early as September 2014, after the programmed year-long shut-down. They have identified two possible sites for the deployment of the SOLi∂ detectors: an area on level C next to beam port H7 (min distance 6.5m) in the experimental hall and on level B in room 42 (min distance 8.5m) where the 1981 neutrino oscillation experiment was installed. We took some preliminary background measurements in december 2012 and January 2013 and the current level at C-H7 is quite high and substantial work is required to shield the beam port which ILL will take on during the shut down. The final background level at the site is therefore not yet known and measurement will have to be repeated when ILL restart. On Level B42, the reactor background is highly suppressed but the area on the ground is busy with a large deuterium tank, pumps and pipes running along the reactor walls. The SOLi∂ detector will have to placed higher up, close to the ceiling.
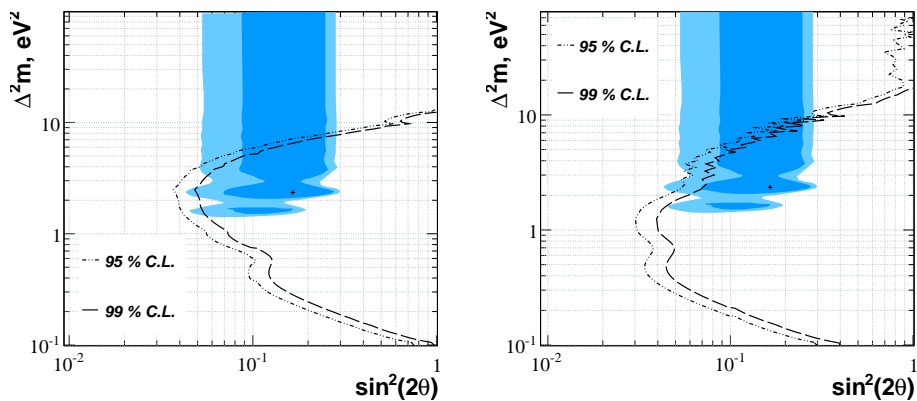
Figure 15: (left) Example of sensitivity curve obtained close to the H7 beam port on level C. (right) Example of sensitivity curve close to the ceiling on level B in room B42 for the same statistical power as on the left.

- **BR2**: the BR2 reactor is essentially used for irradiation of materials in or close to the core by the silicon industry and medical research. The main beam ports are vertical ones leaving room for approaching instruments near the walls around the reactor core. The minimum distance of approach is 5.5m with minimal constraint of space and time for a two-year measurement time. The BR2 is also expected to stop for a long period of time between the end of 2014 and most of 2015. The reactor background level is minimal with environmental level of neutrons and low to medium level of gamma-ray radiation. These conditions are likely to remain unchanged for a deployment there as no measurement are taking place on level 10m67.

Although C-H7 and B42 are available for the experiment at the ILL, SOLi∂ is in direct competition with STEREO for the level C area. After a review of both proposals in march2013, the Scientific council of ILL has decided to give priority to the STEREO proposal on level C if the experiment is funded. In this scenario, B42

will be used for the SOLi∂ experiment but additional funding for providing the metallic structure will have to be sought from new collaborators or drawn from contingency. Moving to the site at BR2 will be considered in the future (in 2016) to pursue the oscillation measurement in the higher mass region and for non-proliferation studies. It will be used also for measurements with the SOLi∂ prototype system during the summer or fall 2013.

A summary of the important parameters for both reactor sites is shown in table 3.

Table 3: Important parameters for both reactor sites considered for the SOLi∂ experiment.

Parameter	ILL-C-H7	ILL-B42	BR2-R1
Power [MW]	58	58	60
Min. distance [m]	6.5	8	5.5
Exposure time d/yr	300	300	125-150
antineutrino rate at min distance [/ton/day]	985	650	1418
Overburden [m.w.e]	12	8	10
Reactor neutron bkg	high	bkg	bkg
Gamma neutron bkg	high	low	low
Shut-down period	Aug13-Aug14	N/A	Sept14-Dec15

6 International Collaboration and UK contribution

The SOLi∂ experiment is a UK-lead collaboration with currently the participation of the CNRS-Subatech group from Nantes, France. The UK responsibility is to provide a fully functional 1.44t detector as well as the electronics and the DAq. Both Oxford and Imperial College London have strong neutrino groups and are well positioned in the analysis of currently world leading experiments like T2K or MINOS. These groups have also a long experience in building the T2K near detector calorimeter modules, electronics and DAq. Oxford has submitted in February a ERC Consolidator Grant at the level of 1.5M to build one SOLi∂ detector system which could greatly help with securing the full amount of funding required for a two detector experiment. The collaboration with CNRS-Subatech is central to the experiment: the Subatech group has already taken the responsibility in the detector sub-module design and will provide the reactor flux calculation. SOLi∂ will benefit from the interdisciplinary knowledge of Subatech researcher in the field of nuclear physics and nuclear reactor evolution codes. Subatech is also leading the development of the detector sub-module in France and has submitted a proposal ANR Jeune Chercheur in January 2013 to build one of the sub-module early on (249k Euros). A few more CNRS laboratories have shown a strong interest in the experiment and we are currently aiming at expanding the number of European group involved. A second opportunity to attract funding in France will open this summer where a presentation of SOLi∂ experiment made at the IN2P3 Scientific council.

7 Work Package 1 : Management and Travel

7.1 Project Management

The soLi∂ construction project will be managed by a project management committee (PMC) made of the work package managers and lead by a project manager . Their participation to the committee is key to ensure a good coordination of effort between all institutes as most individuals have pre-existing experience of collaborating with each other. Vacheret has spent many years at Imperial College and was a work package manager for the T2K ECAL project. He has build a very good relationship with technical staff there which will facilitate the management of the effort at both institutes. Nash, as the High Energy Physics group leader at Imperial College London and holder of the Consolidated Grant, will help with the allocation of resources required for the project. A. Weber has a long experience in managing electronics development in Oxford and RAL with Vacheret on T2K. Fallot and Vacheret are already benefiting on pre-existing collaboration on developing new tools for reactor monitoring (through a J. Fell Fund award) and Subatech, Imperial and Oxford have already regular meetings on the development of the mechanical design.

Table 4: WP1 manpower

Individual	Task	SY				PPRP
		FY1	FY2	FY3	total	
University of Oxford						
A. Vacheret	member of PMC	0.1	0.2	0.1	0.4	0
A. Weber	member of PMC	0.04	0.09	0.02	0.15	0
Imperial College London						
J. Nash	member of PMC	0.025	0.05	0.025	0.1	0
CNRS-Subatech						
M. Fallot	member of PMC	0.05	0.05	0.05	0.15	0

7.2 Travel

The travel required for soLi∂ is fairly substantial and is divided into the following items :

- visits to detector component suppliers

- visits to the research reactor site

- Testing campaign for the prototype

- installation of the detector modules

- Commissioning period of the detector

- Collaboration meetings

A eight day test campaign at the BR2 reactor in Mol is planned to make a first measurement of antineutrinos with the prototype and a comprehensive measurement of the atmospheric and reactor background at the site. The campaign will require two people to install neutron and antineutrino systems and commission it prior to the restart of the reactor in Aug 2013 or October 2013. Two visits respectively to the supplier covering mainly the period of production of the carbon fibre tray and electronics board is foreseen. In order to facilitate the preparation of the detector site (background measurements, shielding...) near the reactor, two short visits are required for two people. The installation and commissioning of the detector module requires the mounting of the shielding enclosure which is a highly time consuming task as well as the installation and cabling of all modules. This phase requires most of the experts to be on site for a period of three months. To help with the preparation of the site and installation we also require two weeks of travel for two technicians. Two collaboration meetings per year are necessary (total of 4 meetings) to make steady progress on all the aspects of the experiment and ensure a smooth integration of all the components. Each institute is foreseen to host the meeting and this will require an average of 6 people travelling in the UK, France and Belgium.

The working allowance take into account a possible decrease of the currency rate from GBP to Euros of 10%. Contingency include the possibility of delay in assembling the detector translating in a longer installation and partial commissioning period which will have to be extended by another two months.

Table 5: WP1 Requested Travel Funds

Purpose	Cost/visit	Length (days)	Visit	total (GBP)
Visits suppliers	500	2	4	2,000
Visits reactor	600	3	4	2,400
Test at BR2	1,700	14	2	3,400
Installation Detector	1,700	14	2	3,400
Commissioning Detector	9,300	90	5	50,300
Collaboration meetings	600	3	24	12,000
Total				**71,700**
WA				6,800
Contingency				31,000

8 Work Package 2 : Detector construction

8.1 Institute responsible

This work package will be provided by the University of Oxford (Sub-department of Particle Physics) and Imperial College London (High Energy Physics). The work package manager is Vacheret.

8.2 key personnel

- **G. Barber, Imperial College London**
  Barber is a Mechanical engineer, he has worked in Hep for more than 30 years. Responsible for the Cern NA14 silicon detector in the 1980s. Was part of the design, build and installation of the Inner Tracking Chamber for the Aleph Experiment at Cern. Responsible for the inner region of Aleph during the silicon tracker upgrade. Worked on the CMS ECal and is now currently involved with the Mice Experiment at Ral with responsibility for the design development build and installation of the scintillating fibre trackers.

- **J. M. Buhour, CNRS-Subatech**
  Jean Michel BUHOUR has been Research Engineer (CNRS position) at SUBATECH/Ecole des Mines de Nantes (France) since 2006 and at the IPNO laboratory between 1996 and 2005. He graduated in mechanical engineering from BREST University (France) in 1994. From 1996 to 2002, he work as mechanical Engineer and mechanical simulation expert at the IPNO (LHC, CPO protonthrapie project), he become the head of the mechanical department of IPNO in 2003. During the last 7 years, he was participating in several projects at SUBATECH involving his competences in mechanical design; mechanical, thermal and fluidic simulation (MYRRHA, THERANEAN, Radionuclide research and production and the MFT a possible ALICE upgrade). He is the head of the mechanical department of SUBATECH (14 people) since 2011.

- **G. Guilloux, CNRS-Subatech**
  He is an expert engineer in mechanics. He has worked in numerous international particle and nuclear physics experiments (NA14 @ Cern, ALEPH@ the LEP, CLIO, VIRGO, SPIRAL@GANIL, STAR @BNL USA, the cyclotron ARRONAX of Nantes). He has created the mechanical service of the SUBATECH lab. at the creation of the laboratory in 1994. The project will benefit to a large extent of his skills in mechanical study, design, and construction. This project completes also his skills in the domain of scintillator detectors. Grard Guilloux is working on the sub-module mechanical design. He is motivated by this responsibility and appreciates to learn new abilities.

- **P. Scovell, Oxford**
  Scovell has experience in working on the development and physics exploitation of liquid noble gas detectors for dark matter searches in the ZEPLIN-III and XENON100 experiments, contributing to more than 20 international publications. He also has experience in the development and commissioning of large scale solid-state radiation detection systems including design, simulation, electronics development and data analysis. He has been at the University of Oxford for the past 12 months working on the MARS neutron detector project whilst developing the simulation package for the SOLi∂ detector.

- **A. Vacheret, Oxford**
  Vacheret has an an extensive expertise in the design, optimisation construction and test of various

calorimeters including the T2K near detector one. He was the photosensor work package manager on the T2K calorimeter project and has an excellent record for delivery. He has spent nearly seven years working with new solid state avalanche photo-sensors. He developed the scintillator detectors calibration methods and convened the calibration group effort for the first T2K analysis. Now as STFC advanced fellow, he is a T2K analysis convener and started the MARS project to develop next generation systems dedicated to the detection of neutron and neutrinos for science and applications. His domain of expertise ranges from detector concepts, scintillators, photo-detectors, front-end electronics and simulations.

8.3 Introduction

The soLi∂ detector is based on cubic scintillator element read out by a network of optical fibres. The detector consists of five sub-modules, each made of four layers of 1.2 m x 1.2 m x 0.22 m containing 576 PVT scintillator cubes, 48 1.25 m wavelength shifting fibres. The total number of PVT cubes is 11,520 and the fibres are read out on both ends by solid-state multi pixel photon counter (MPPC). The total number of electronics read out channels is 1920. Each sub-module can be viewed as individual detector unit and will be composed of four layers or cube trays. A exploded view of the tray is shown in figure Figure 16 with the tray holder cubes and WLS fibres.
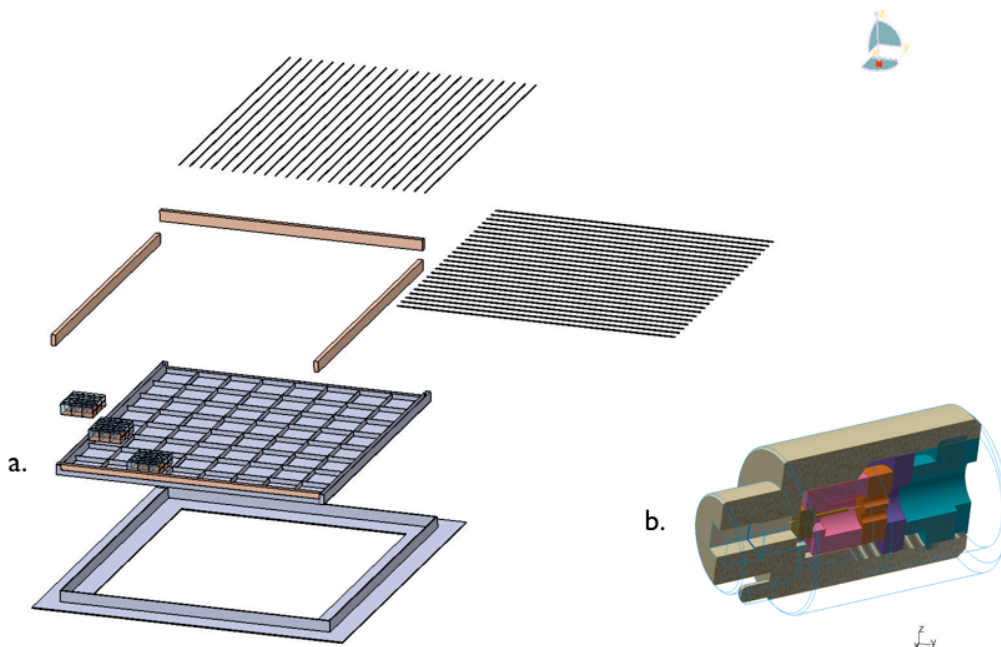
Figure 16: (a.) Exploded view of the current carbon fibre tray with cubes, WLS fibres and HDPE reflectors. (b.) MPPC-fibre coupler design for 3 mm x 3 mm MPPCs.

This partitioning simplifies the construction process but also the handling of the detector for testing and shipping calibration and installation on site. The full scale detector had a total fiducial mass of 1.44 tonnes. The front-end electronics will be installed inside the sub-module and the DPC cards on a shelve unit installed at the back of the last module. The connector to couple the MPPC to the fibre is being designed and prototyped with 3D printing prior to the start of the project. This connector will be produced in large quantity by plastic mould injection.

8.4 Inputs

In order to meet the commitment of this work package the following inputs are required

- Provision of connector and ferrule design (Oxford)

- Provision of photosensors attached to electric cable and tagged (WP3)

- Provision and support of DEIMOS front-end boards (WP3)

- Provision of the DAQ (WP3)

- Provision of a detailed design of the reactor site (Research Reactor personel)

8.5   Objectives and Milestones

The tasks of constructing of the SOLi∂ detectors is shared between Oxford and ICL. Both institutes will share the tasks of constructing the sub-modules to keep the construction phase to a reasonable length. The objective of this work package is to deliver a fully functional detector for the SOLi∂ experiment.

8.5.1   Task 1: Design of the SOLi∂ detector and shielding enclosure

Barber will be providing the full design of the SOLi∂ detector. The detailed conception of the layers and sub-module is ongoing at CNRS-Subatech and will continue until the start of the project. The full design to be delivered in this work package will include the preliminary work done at Subatech as well as the design of the external shielding enclosure surrounding the detectors. The work prior to the start of the project will also benefit greatly from the experience gained in the construction of the prototype module at Oxford during summer 2013. The coordination of the work will be facilitated by the regular meetings already taking place on a biweekly basis between Imperial, Subatech and Oxford. The Design of the detector system will start at the beginning of the project and will take three month for completion. A independent review of the design will take place to validate it at the end of the third month prior to placing the orders.
   A critical part of the design is the scintillator cubes tray and the design will have to include :

- The design of the carbon fibre tray with all of the jigging

- The testing of the tray to ensure there is acceptable deflection when loaded.

- The fibre routing designed in such a way as not to place undue stress into the light guides during and after assembly.

- Inclusion into the tray bosses/brackets to accurately fit the MPPC units.

- Modularity of the trays so that as many components as possible are identical to minimise development work.

8.5.2   Task 2: Preparation of the detector parts

Production of the PVT cubes : The cutting and machining of the cubes to dimension will be performed at Oxford using the CNC machines. In order to produce 12,000 cubes for the detector around 50 PVT slabs (5 cm x 55 cm x 200 cm) will be saw cut in small cubes. The cubes and their groove will be machined with tight tolerances. The current capacity of the Oxford Mechanical workshop enable a rate of production of around 500 cubes per week allowing for a completion of production in about eight months time. Experience on machining the cubes will be drawn from the construction of the 64 cubes prototype to be build during the May-June 2013 period in Oxford.
   Production of MPPC connector and ferrule parts : the design of the connector, small production using 3D printing and test will be completed prior to the start of the project at Oxford. For the large scale production of connectors, plastic injection moulding will be used to achieve high precision manufacturing at low cost. Twenty five days of Mech. Design. Eng. at Oxford will be needed to supervise the production and delivery of the connector parts and the design of a few jigs for assembly tasks.
   Preparation of cubes : this task comprises the cutting of the ^{6}LiF:ZnS layer to the size of the cube face and gluing it on top of the cube using controlled amount of epoxy glue. This task is critical to the performance of the detector system and will have to be done for every single cube. Once cured, reflective coating (Tyvec or Ti02 paint) will be applied. Jigs for gluing and cube painting will be designed and prepared both at Imperial and Oxford to facilitate the task and to achieve a rate of around 300 cubes ready to assemble per week. Scovell and a technician will take care of this task at Oxford. PDRA1, Casey will take on the task at Imperial.
   Preparation of fibres : The fibre end will be trimmed with diamond cutter to appropriate length and will be done in bundles. Jigs will need to be designed that ensure that the fibres are held rigid so as not to allow any vibration in the fibres and cause poor surface finish. Ferrule on one end will be glued once fibres are polished. Barber will coordinate the polishing with the Imperial Mechanical workshop.

Mounting MPPC onto connector : MPPCs with their cables will be mounted onto the plastic connector piece and labeled. The MPPC package chosen has two pin which can easily receive standard pins socket to facilitate the connection to cables and Deimos cards. A picture of the MPPC that will be used is shown in Figure **??**. M. Khaleeq and a fraction of PDRA1 at Imperial will take on this task as well as Scovell and Electronics technician in Oxford.

8.5.3   Task 3: Sub-module Assembly

Once enough of the detector parts are produced and prepared the assembly of layers will commence.

Layer assembly : the carbon fibre tray will be placed and filled with ready-made cubes properly aligned in position (using metal rods with same section as fibre). Neutron reflector panel will then be put in position and fibres inserted in grooves. The second ferrule will be glued on the opposite end of the fibre. A foam layer will be added on the top to keep cubes in place and a cover will be placed to isolate the layer. At this stage a first check of the layer uniformity can be performed using a calibration source or cosmic-ray muons with a standard CAEN digitiser unit or if available a first test system based on the electronics developed in WP3. We estimate that it will take around four months to assemble the first layer and then between two and three weeks once the first module is build.

Sub-module assembly : The layer will be moved (whether with a crane of by personnel) to the main sub-module assembly area. Once the four layers are in place photosensors with cables will be mounted on the ferrule. The Deimos board will be installed on the main frame and MPPC connected to each board. Data and power cables will then be connected to external ports and power lines. Finally a cover in carbon fibre will be placed on top of the layer. Two additional reflector panel in HDPE will be installed on the top and bottom modules. The first module will take 5 months to build and the other expected to take 3 months. For the detailed milestones of the submodule assembly see table 8.5.7.

Sub-module testing Some preliminary test at each institutes will be conducted with a DPC card based test system. Test with radioactive sources and cosmics will be performed to check the uniformity of response of the system. These tests will take a few days using analysis package developed for the prototype to automate the task.

8.5.4   Task 4: Neutron efficiency calibration and response characterisation

The first two modules build will be carried over to the National Physical Laboratory (NPL) to perform a absolute calibration of the neutron efficiency using a precisely known neutron beam and various sources to check and fine tune the trigger to gamma-neutron coincidences. These modules will be use as reference for the inter calibration of the remaining modules. Five days of beam time are required for this test.

8.5.5   Task 5: Shipping of submodules at reactor site

Each sub-module will be built and tested at respective institutes with test systems provided by WP3. Once the Quality assurance is preformed they will be shipped to the reactor site for installation.

8.5.6   Task 6: Commissioning of the detector

The commissioning phase will start once the modules are shipped on site and installed in front of the reactor. The commissioning will require all experts to spend a few months on site to test the hardware, commission the DAQ and electronics with the full system in place and develop the in situ calibration.

8.5.7   Milestones

Name	Definition	Date
WP2M1	finalise detector and shielding enclosure design	Nov 2013
WP2M2	complete sub-module 1 at Imperial	Jun 2014
WP2M3	complete sub-module 2 at Imperial	Sep 2014
WP2M4	complete sub-module 3 at Imperial	Dec 2014
WP2M5	complete sub-module 4 at Oxford	Jun 2014
WP2M6	complete sub-module 5 at Oxford	Sep 2014
WP2M7	beam test at NPL	Oct 2014
WP2M8	Commissioning of complete detector at reactor	Jan 2015

8.6 Output

The deliverable of this work package is a fully functional 1.44T fiducial mass detector system.

8.7 Resources Requested

To achieve these goals we need the resources summarised in tables 6 and 7.

Table 6: WP2 manpower

Individual	Task	SY				
		FY1	FY2	FY3	total	PPRP
University of Oxford						
A. Vacheret	WP Manager	0.2	0.4	0.2	0.8	0
P. Scovell	Assembly at Oxford	0.4	0.9	0.3	1.6	1.28
Mech. Eng.	jigs design at Oxford	0.25	0	0	0.25	0.2
Imperial College						
G. Barber	Leading Mech. Design	0.25	0.33	0	0.58	0
PDRA1	Module construction & tests	0.5	1	0.5	2	1.6
M. Khaleeq	Module assembly	0.1	0.24	0	0.34	0
V. Casey	Module assembly	0.1	0.24	0	0.34	0
Mech. Workshop	Mech parts & jigs	0.1	0.24	0	0.34	0.2
SubaTech						
J. M. Buhour	Leading module Mech. Design	0.15	0	0	0.15	0
G. Guilloux	Sub-module design	0.15	0	0	0.15	0
Total		2.2	3.35	1.0	6.55	**3.28**
WA		0.1	0.45	0.05	0.6	0.48

The contingency estimated in table 7 is to account for having to rebuild a submodule entirely (100k). This could happen for instance in the case of a flaw in the design or an incident with a module during transportation. It accounts also for the possibility of having to provide the metallic structures for mounting the detectors in level B42. This could happen if no additional collaborator is found for this contribution.

Table 7: WP2 consumables and equipment

Item	Quantity	Price/unit	total (GBP)
PVT Slabs	50	2,200	110,000
Neutron screens	120	868	104,112
WLS fibres	1,200	29	34,963
MPPC connector	2,300	8	18,000
HDPE Shielding	20	2,125	42,500
Carbon fibre tray	22	2,363	52,000
mechanical parts			12,000
Various consumables			8,000
Shipping cost	5	1000	5,000
Test at NPL	5	2500	12,500
Total			**399,075**
WA			40,000
Contingency			150,000

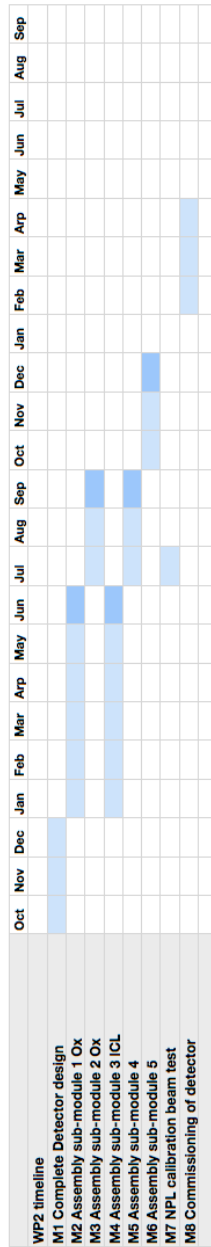|	Oct	Nov	Dec	Jan	Feb	Mar	Arp	May	Jun	Jul	Aug	Sep	Oct	Nov	Dec	Jan	Feb	Mar	Arp	May	Jun	Jul	Aug	Sep
WP2 timeline																								
M1 Complete Detector design																								
M2 Assembly sub-module 1 Ox																								
M3 Assembly sub-module 2 Ox																								
M4 Assembly sub-module 3 ICL																								
M5 Assembly sub-module 4																								
M6 Assembly sub-module 5																								
M7 NPL calibration beam test																								
M8 Commissioning of detector																								

Figure 17: WP2 Gantt Chart.

9 Work Package 3 : Electronics and DAQ

9.1 Institutional Responsibilities

The University of Oxford (Sub-department of Particle Physics) will take the lead in this work package. It is supported by Imperial College London which will provide a firmware programmer to develop the data reduction and triggering capabilities of the backend electronics and SubaTech, who will contribute to testing and commissioning.

9.2 Key personnel

The following people are central to this work package:

- **A. Weber, Oxford & STFC/RAL**
  Weber has a long history in instrumentation in neutrino physics from MINOS and T2K. He lead the production of the far detector front end electronics and timing and trigger system for MINOS and also was in charged of co-ordinating the electronics for the entire ND280 near detector. He co-designed and delivered the electronics for several of the T2K near detectors and the overall timing and trigger system. He leads this work package.

- **A. Baird, Oxford**
  Baird is an experienced electronics engineer who has worked at RAL and Oxford for more than 10 year, designing and building electronics in particle physics and beyond. His experience spans a large variety of applications from high current to RF to DAQ applications. He developed data acquisition board for SKA and RF amplifiers for LOFAR and was central for the success of BDOT a device to measure magnetic field disturbances in NIF. He started the development of electronics prototypes for SoLi∂ and will drive future development and implementation.

- **N. Ryder, Oxford**
  Ryder is a enthusiastic and excellent young researcher, who previously worked on large scale experiments (ATLAS, CMS and the ILC) as well as on small scale demonstrator projects. He has developed a DAQ system for an experiment testing optical fibres at a nuclear facility and also worked on ATLAS' DAQ system. He was awarded a Junior Research Fellowship to work on SoLi∂ and to develop the DAQ.

- **A. Rose, Imperial**
  Rose is a physicist and electronic engineer of the High Energy Physics group at Imperial College. He has day-to-day responsibility for hardware design, commercial manufacture and remote operations and studies of CERN-based systems. He designed and implemented the CMS Level-1 trigger and as a result he is highly expert in online and offline software, with excellent firmware and hardware skills. Rose has previous experience of the CMS upgrades project, this involved work in C++, python, VHDL and Verilog. He has also constructed systems that demonstrate all the key technologies required for a future trigger architecture, including processing and infrastructure hardware, high-speed optical interconnections, readout pipeline architectures, algorithms and full software and firmware chains.

9.3 Introduction

As described in previously, the scintillation light from the interactions in the detector is captured by 3×3 mm^2 square WLS fibres and guided to matching MPPCs. These MPPCs are operating at a gain of around 10^6 and are read out by an electronics/DAQ system that has started to be developed by the University of Oxford.

The SoLi∂ electronics & DAQ system is build around a commercial 12-bit, 4 channel, 80 MHz ADC that continuously digitises the data from the photo detectors.

The signals from the MPPCs are connected to a dedicated front end card (Deimos), which has several functions: supplies the MPPCs with their individually adjustable voltage, amplifies their signals and drives them to a differential ADC located on the Digital Processing Card DPC (see blow) and also provides a charge injection capability to calibrate the electronics. Deimos is a largely passive card connected to 32 MPPCs. 2 (or 1) Deimos card are connected to a DPC.

The DPC is the hard of the system, it continuously digitises the data from the MPPCs, using its on-board ADCs. The ADCs are controlled and send their data to a SPARTAN 6 Field Programmable Gate Array (FPGA) from Virtex. This FPGA is the heart of the system. It zero suppresses the data, putting all significant hits into a ring buffer, which should be able to hold data for several hundred μsec. At the same time it looks for a neutrino signature, which is a distinct several μsec long pulse. Once it found this signature, it will communicate this

information (via a token ring) to the other DPCs and all DPCs will write the data in the ring buffer to the DAQ. In the same way one can record pedestal events (using random triggers), calibration triggers and cosmics (looking for a distinct hit pattern in a single card). The timing of the different cards will be synchronised using a common clock and regular time synchronisation signal. A high level overview of the system can be found in figure 18.
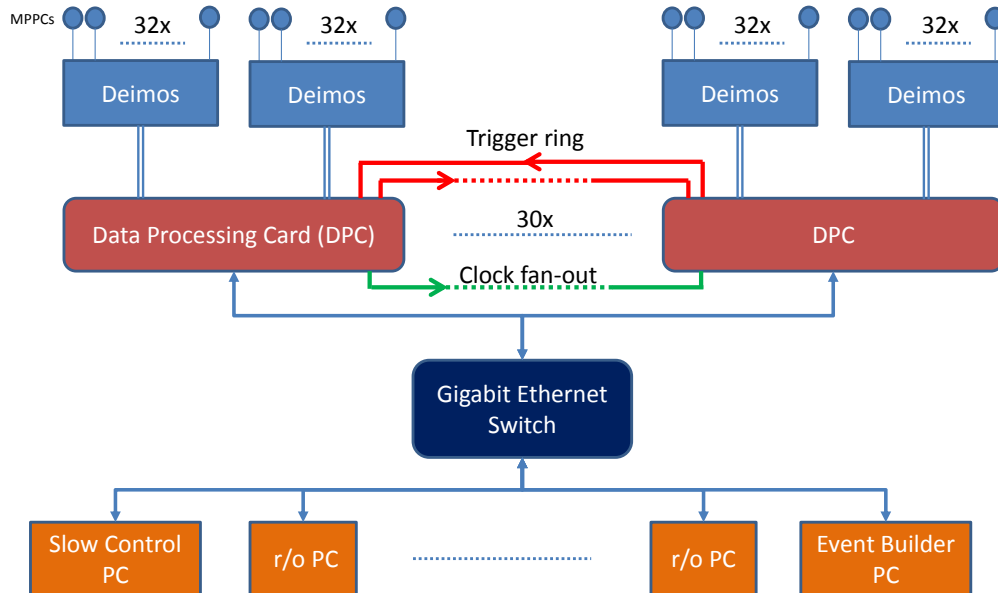
Figure 18: **Overview of the electronics and DAQ system**

9.4   Inputs

The performance of the detector and the optimal way of extracting the signal over the large background depend in a substantial way on the design of the electronics, the triggering and the DAQ capabilities. As such there is a substantial interplay in the initial design phase between the detector optimisation and the detailed definitions and specification of the electronics. The detailed inputs are:

- requirements for detector triggering and readout window
- signal pre-processing and data reduction requirements (depend on details of data analysis requirements)

9.5   Objectives and Milestones

9.5.1   Task 1: Development of 32 channel DPC Prototype

We have already build the hardware for a 32 channel DPC prototype and are currently in the process of verifying the board and to develop the firmware for digitising and data processing as well as data transfer to PC via Gigabit Ethernet. This work has to finish. Especially the full card verification and the firmware development for data processing will continue.

9.5.2   Task 2: Develop 32 Channel Deimos Card

We have already started he schematics and layout for the frond end card that amplifies the MPPC signals and drives them to the DPC. A prototype of the card has to be produced and tested with the DPC. Once certified the full batch will be produced and tested in Oxford using the DPC prototype.

9.5.3 Task 3: Test-system DAQ development

The prototype DAQ system that interfaces with the DPC via Gigabit Ethernet is relatively straight forward as the number of channels is limited. The main task is to set-up the DPC and Deimos cards and to retrieve the digitised data after basic triggering. This system will be used for component testing during construction.

9.5.4 Task 4: Develop final DPC

The plan is to increase the number of digitisers on the DPC from the current prototype with 32 channels to a total of 64 channels. (64ch baseline) An improved version of the board will be produced. This will reduce the total cost of the system. Furthermore the full trigging and data reduction functionality have to be developed. This will be done in collaboration between Oxford and Imperial.

9.5.5 Task 5: Produce Final DAQ and Electronics System

We have to fully specify the requirements, especially bandwidth and deadtime, for the DAQ system. Following from the system layout will be determined and implemented. Front end DAQ processes to read out the DCP will be finalised based on the work started in Task 3/4.

9.5.6 Task 6: Commission electronics/DAQ

A large part of the system will be commissioned to readout the sub-modules just after production. Final commissioning will happen on the reactor side after installation.

9.5.7 Milestones

Name	Definition	Date
WP3M1	verify basic operation of Deimos and DPC	Oct 2013
WP3M2	finish final version of DPC	Dec 2013
WP3M3	prototype test system available for testing	Mar 2014
WP3M4	finish design of DAQ/DCS	Apr 2014
WP3M5	finish production of Deimos	May 2014
WP3M6	finish production of DPC	Sep 2014
WP3M7	electronics/DAQ system available for commissioning	Jan 2015

9.6 Resources requested

To achieve these goals we need the resources summarised in tables 8 and 9.

Table 8: WP3 manpower

Individual	Task	SY				PPRP
		Y1	Y2	Y3	total	
University of Oxford						
A. Weber	WP Leader	0.15	0.25	0.05	0.45	0
A. Baird	Lead Electronics Engineer	0.1	0.2	0	0.3	0.2
E.Eng	DPC/Deimos development	0.25	0.75	0.	1	1
Elec. Technician	DPC/Deimos layout, assembly and testing	0.2	0.7	0.1	1	1
N. Ryder	DAQ& electronics Interface	0.5	1	0.5	2	0
P. Scovell	MPPC spec and testing	0.05	0.1	0.05	0.2	0.2
Imperial College						
A. Rose	DPC firmware development	0.15	0.2	0.15	0.5	0
SubaTech						
A.N. Other	DAQ and electronics commissioning and testing	0.0	0.4	0.3	0.7	0
WA	working allowance	0.15	0.25	0.1	0.5	0.5

The contingency noted in Table 9 is dominated by additional resources needed, if DPC is limited to 32ch only. This would requiring doubling the number of DPCs with only a slightly smaller coster per DPC.

Table 9: WP3 consumables and equipment

Item	Quantity	Price/unit	total (GBP)
MPPC	2000	39$	59,000
& cables	2000	3.5$	7,000
prototyping			5,000
DEIMOS	65	700	45,000
DPC(64)	35	2,500	87,500
PS	4	1500	6,000
PCs	10	800	8,000
network			5,000
sundries			5,000
Total			**227,500**
WA			10,000
Contingency			70,000

9.7 Output

The output of the work package is in general terms an electronics and DAQ system that allows for the testing, calibration and data taking of the detectors. In more detail they are:

- building of prototype Deimos board and DPC to be used for detector testing

- production of Deimos board and DPC including cabling and power supplies

- electronics/DAQ and detector control system to readout detectors

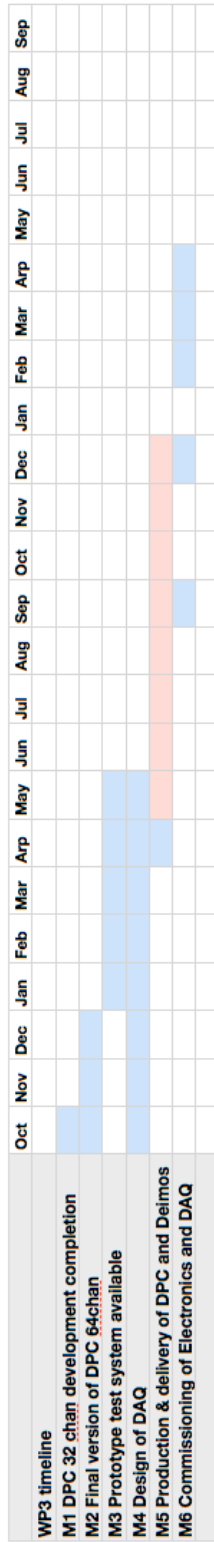| WP3 timeline	Oct	Nov	Dec	Jan	Feb	Mar	Arp	May	Jun	Jul	Aug	Sep	Oct	Nov	Dec	Jan	Feb	Mar	Arp	May	Jun	Jul	Aug	Sep
M1 DPC 32 chan development completion		▓																						
M2 Final version of DPC 64chan			▓																					
M3 Prototype test system available							▓	▓																
M4 Design of DAQ							▓	▓																
M5 Production & delivery of DPC and Deimos								▓	▓	▓	▓	▓	▓	▓	▓									
M6 Commissioning of Electronics and DAQ												▓			▓		▓		▓					

Figure 19: WP3 Gantt Chart.

10 Work Package 4 : Reactor flux calculations, detector simulation and optimisation

10.1 Institute responsible

CNRS-Subatech is responsible for this work package.

10.2 Key personnel

- **M. Fallot, CNRS-Subatech**
  M. Fallot is the work package manager. She is an assistant professor at the University of Nantes since September 2003. She has a long experience as nuclear physics experimentalist and work for many years at at Ganil, GSI, ILL, CERN ISOLDE and Orsay Tandem. She is leading the Double Chooz and Nucifer group at SUBATECH since 2004-2005. She is also co-leader of the reactor and anti-neutrino simulation working group, which has led to the neutrino prediction used in the Double Chooz θ_{13} papers. She is also leading the Experimental Research on Data, Reactors and Energy (ERDRE) group at SUBATECH and conduct experiments to refine the calculation of reactor energy spectra. She coordinates the sub-WG devoted to neutrino detection created by the Novel Approaches-Novel Technologies (H. Toivonen, STUK) European Safeguards R&D Association (ESARDA). Her interdisciplinary profile and wide expertise is a strong asset for the success of the project.

- **L. Giot, CNRS-Subatech**
  L. Giot is an assistant professor at the Engineering School Ecole des Mines de Nantes (EMN /SUBAT-ECH) since 2007. L. Giot is the head of the engineering program on Reactor plant design and operations at the school. Lydie worked at the Gesellschaft Fr Schwerionenforschung(GSI) on of the fission and spallation processes in the context of accelerator driven systems. She worked at the GANIL and GSI accelerator facilities where she developed skills in experimental nuclear physics, analysis of multi-parameter experiments and low energy nuclear theoryShe made key contributions to the Double Chooz and Nucifer experiments on the reactor core simulations developed with MCNP/X and MURE (Takahama Benchmark, PWR assembly simulations, Osiris reactor). She has took in charge complex MCNPX simulations of the gamma-ray background for the Nucifer collaboration. In this project, L. Giot will take on the ILL reactor simulation with MURE and the dedicated gamma-neutron background studies. The SOLi∂ experiment will give her the opportunity to deepen the skills she acquires in reactor simulations.

- **P. Scovell, Oxford**
  P. Scovell has been a PDRA at the University of Oxford since May 2011. He studied for a PhD at the University of Edinburgh as part of the ZEPLIN-III dark matter experiment. His thesis covered the analysis of both dark matter searches and the design, commissioning and analysis of a tonne-scale solid-state veto detector. Upon completion of his PhD in 2010, he moved to the University of California, Los Angeles to work on the XENON100 dark matter detector. He has build knowledge in the development and commissioning of large scale solid-state radiation detection systems for the MARS project including design, simulation, electronics development and data analysis. He has developed the SOLi∂ detector GEANT4 simulation and the current optimisation studies for the mechanical design. He will manage the detector simulation package required for the Monte Carlo simulation of the detector response in conjunction with the reactor flux calculations. He will also manage the development of event visualisation software which will include a data reduction package capable of analysing both real and simulated data in parallel.

10.3 Introduction

This work package addresses the challenge of providing a accurate calculation of the anti-neutrino flux and detector response to understand with great precision the data taken at the research reactor. These calculations are central to the motivation of this proposal and coupled to a well understood detector simulation, is expected to provide a robust reference anti-neutrino flux used for future neutrino experiments. The Monte Carlo simulations will also be used to accurately determine the background from reactor and the environment surrounding the detectors.

10.3.1 Reactor flux calculation

A detailed simulation of the reactor is mandatory for the calculation of the expected anti-neutrino spectrum and flux, that can be used for reference calculations to compare with the measurements in both SOLi∂ detectors. Such detailed reactor simulations have already been performed by Subatech in the Double Chooz experiment and the Nucifer experiment, providing the fission rates at the origin of where the anti-neutrinos are emitted. The simulation of the ILL core will be performed following the same methodology using the MCNP Utility for Reactor Evolution (MURE) code. Subatech has now a good control of the systematic errors associated to such reactor simulation and its key input parameters, thanks to the work done as part of the Double Chooz collaboration.

10.3.2 Detector simulation and optimisation

The simulation of the SOLi∂ detector has been developed using simulations from both the T2K [16] and ZEPLIN-III [17, 18] detectors. The simulation has been developed using the GEANT4 package and is fully customisable in order to investigate various configurations at both the full detector and single cube geometry levels. The simulation includes the capability to track photons from the interaction point via absorption and re-emission in the wavelength shifting fibre to the MPPC surface. Photons which are absorbed at the MPPC surface are converted into an expected signal waveform using a simulated MPPC response which includes after-pulsing, pixel cross-talk and a basic modelling of the response of the DAq system (including DAq sampling rate and dynamic range). The final goal of the detector simulation is to provide a package which uses inputs from the reactor simulation to predict the signal level in the SOLi∂ detector and inputs from background studies to predict the background level in the SOLi∂ detector. Matching of data and Monte Carlo will allow the most accurate measurement of anti-neutrino flux.

The initial goal of the SOLi∂ simulation was to optimise the detector design. This optimisation is gained by considering both data quality, construction practicalities and cost. In order to develop an optimised design, the following points were considered:

- Individual cube light yield - This is considered one of the key objectives of the optimisation process and is influenced by several factors. To investigate this parameter, a variety of configurations were studied that looked at fibre location within a cube (*i.e.* drilled holes through the centre and groves machined on the edges), fibre size, cross-sectional shape and number of fibres (*i.e* individual fibres or bunched arrays) and single vs. double ended readout.

- Neutron capture - there are two major parameters which influence the efficiency of neutron capture on ^{6}Li, the amount of ^{6}Li used and the distance between sheets. Studies have been performed into the optimisation of both these parameters including the optimisation of layer thickness and cube size. Both of these considerations have a large impact on the data quality, the cost and ease of construction.

- Energy response - The size of cube and light-yield directly affect the energy response of the SOLi∂ detector to IBD positrons. The response to positrons of various energies has been investigated for the various configurations designed and acts as an input to the eventual optimised detector design.

Figure 20 shows the optimised layout which will be used as the benchmark design in the SOLi∂ detector. This layout includes a single 3 mm square fibre imbedded into a groove on the sides of each cube perpendicular to a single layer of ^{6}Li of thickness 250 μm. The system will include double-ended fibre readout. Each cube will be covered in a layer of reflective material such as PTFE or Tyvek.

Individual cube response is determined using the response of a single cube to muon interactions. The single MPPC response to muons is shown in Fig 21 and is compared to a muon simulation of a single cube to give a true to simulated light-yield conversion.

In order to determine the true response of the SOLi∂ detector, an individual prototype cube was constructed using the same design as the optimised layout. The light-yield for muons for this cube was determined and is shown in Figure 21. This number acts as an input to the simulation for the determination of the expected response of the full SOLi∂ detector to signal and various sources of background.

10.3.3 Reconstruction

With a model of the detector constructed and the expected light-yield determined, methods for reconstructing the response to various interaction processes have begun to be developed. There are four distinct processes to investigate:
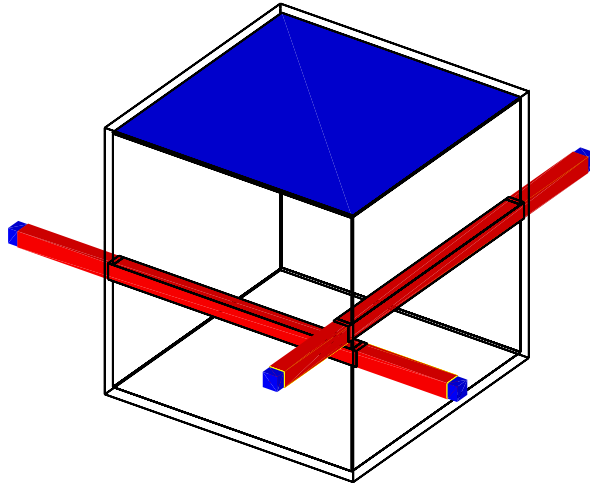
Figure 20: (left) Example configurations for a single scintillator cube in the SoLi∂ detector (see description in text). The ^{6}Li:ZnS is shown in blue, fibres shown in red and MPPC photo-sensors also shown in blue.
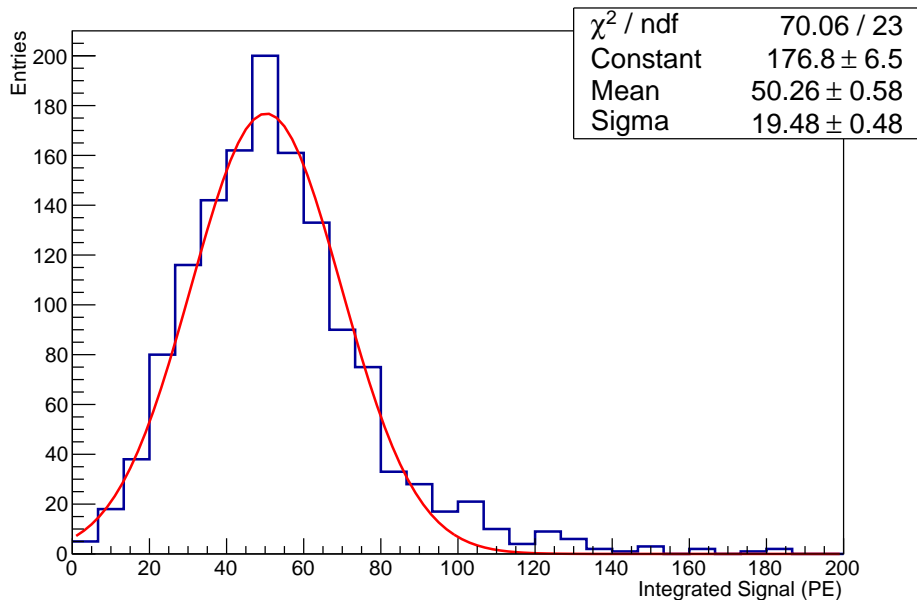
Figure 21: Measured light-yield for muon interactions in a single SoLi∂ cube.

- IBD events - the signal. The detection of inverse β-day involves the detection of a neutron capture on ^{6}Li and energy deposition in the plastic scintillator from a positron.

- Fast Neutrons - neutrons of over 1 MeV of kinetic energy. These events are associated with atmospheric muon interactions and can be reduced using overburden and hydro-carbon shielding. Problematic events are where the neutron interacts through a proton recoil and is subsequently captured by a ^{6}Li, thus mimicking an IBD event. The rate of such events is determined using MARS measurements at ILL.

- γ-rays - the energy profile is determined using germanium measurements at ILL. This kind of interaction can be problematic as it may cause accidental coincidences (when energy deposition from a γ-ray in a single cube is greater than that of a positron) and can smear the energy response of the detector to protons.

- muons - high energy muons will pass through the detector depositing large amounts of energy in many cubes. Such events can be easily identified without the need for a separate muon veto due to a high level of cube multiplicity in the event topology.

In each case, energy deposition is converted into a photon yield which is converted into an expected waveform. All subsequent analysis is performed using the waveform response. In order to boost neutron capture towards the edge of the detector, a 2 cm polyethylene neutron reflector screen surrounds the detector. This screen is, itself, surrounded by 15 cm of borated polyethylene to reduce background from external sources of neutrons. With the addition of this screen, the neutron capture rate increases by 4.0%. The event viewer for a typical IBD capture event is shown in Fig 22. The event viewer shows the spatial profile of the IBD positron and neutron
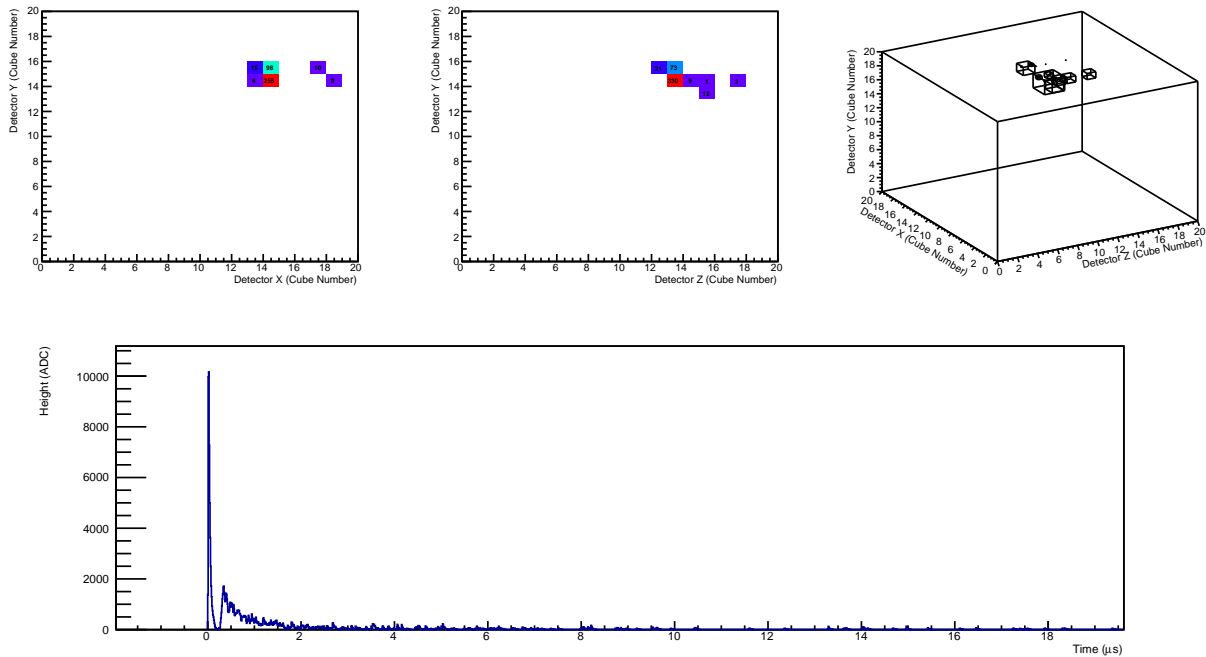
Figure 22: Event view for a typical IBD event in the sOLi∂simulation. At the top is shown (l-r) the light distribution for face 1, face 2 and the 3D representation. At the bottom is shown the sum waveform where the characteristic shapes for the positron and neutron events can be seen.

For IBD events, In data, the neutron will be selected using algorithms loaded onto the fADC boards but it is useful to characterise the expected neutron pulses in order to inform the selection process at a later point. The neutron capture signal has several key characteristics. These include integrated charge, pulse width (both full width and FWHM) and number of individual peaks contained within the signal. Integrated charge is defined as the integral of the waveform above the point of the first detected PE pulse associated with a neutron capture.

With a neutron capture selected, the preceding fraction of the timeline is investigated. In order to minimise the effect of accidental identification of γ-rays as the positron interaction, a geometrical cut is defined. In this case, we demand that the positron interaction occurs within a $5 \times 5 \times 5$ array of cubes. The prompt part of the signal can then be identified by several different methods. Figure 23 shows two of these. The first of these identifies the MPPC pair that contains the largest combined signal within the geometrical cut and the second integrates all signal within the geometrical cut (whilst avoiding double counting).

Figure 24 shows the combination of the visible energy response to neutron capture and positron energy deposition. Neutron capture events will not be selected by energy deposition alone. In addition, parameters such as pulse width and number of peaks (the tail of the neutron capture pulse is formed of a forest of peaks) can be used for selection.

The output from the sOLi∂ simulation also provides a key input for the determination of the true positron energy distribution. Fig 25 shows the comparison of reconstructed and true positron energy. The photon interaction process in the MPPC introduces a small non-linearity in the relationship but this can be easily corrected using the knowledge gained in the T2K MPPC studies. The expected response of the sOLi∂ detector to background signals is discussed in section 3.2.7.
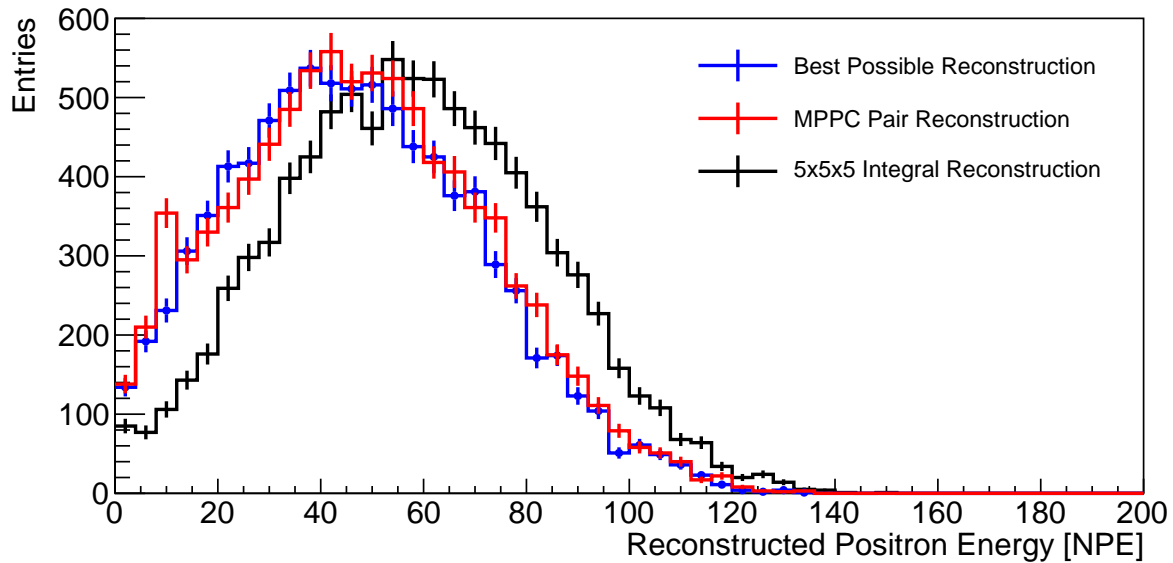
Figure 23: Integral charge for positron events. The blue curve shows the charge calculated using true information about the number of avalanches. The red curve uses the largest MPPC pair within $5 \times 5 \times 5$ cubes of the neutron capture. A contamination (around 10 PE) is seen due to energy depositions from γ-rays. The black curve uses the integrated charge deposition within $5 \times 5 \times 5$ cubes of the neutron capture. As expected, the visible energy is shifted to larger values.

10.4 Inputs

The inputs for the reactor calculation are :

- A detailed geometry of the reactor core and walls from the Research Reactor group

10.5 Objectives and Milestones

The tasks associated to the prediction of the fission rates and the associated emitted anti-neutrinos can be composed of the following sub-tasks :

10.5.1 Task 1: Establish procedure to compute reactor parameters

Establish a procedure to get the main operational parameters of the reactor (i.e. thermal power, boron concentration, control rod positions) during the fuel cycles for the simulation context parameters.

10.5.2 Task 2: Benchmark core simulation

Perform a benchmark between the core simulation done with MURE and simulation results or measurements made at the Research Reactor in order to validate the MURE simulation (observables : fission rates, inventories).

10.5.3 Task 3: Compute systematic errors

Compute the systematic errors associated to the MURE predictions, taking into account the errors associated to the experimental measurements of the input parameters at the Research Reactor (i.e. thermal power error, error on fuel composition at start of cycle, . . .).

10.5.4 Task 4: Correct for context dependent data

Perform basic cross-checks on the input parameters provided by the Research Reactor (to eliminate for instance spurious captor excursions) and on the results of the reactor simulation (total power conservation).
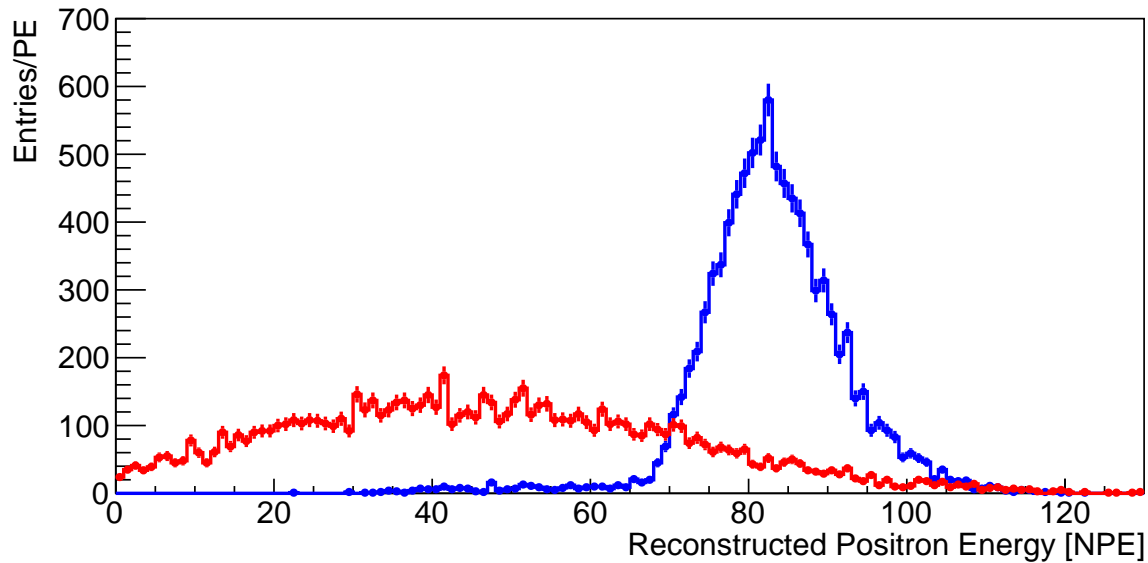
Figure 24: Integral charge for IBD positron (red) energy deposition and ^{6}Li neutron capture (blue) events.

10.5.5 Task 5: Compute anti-neutrino flux and spectum

Compute the anti-neutrino flux and spectrum, including off-equilibrium effects, with the obtained fission rates and the best reference spectra that can be found.
The tasks associated with the SOLi∂ detector simulation are split into the following sections

10.5.6 Task 6 : Input final detector geometry

Reconfigure the simulation to the final total geometry $(1.2 \times 1.2 \times 1)$ m^3 and include modularisation materials (carbon fibre inserts).

10.5.7 Task 7 : Tune detector response

Produce data-sets for calibration runs using sources. A comparison of data and MC will determine the response of the detector to γ-ray, neutron and muon interactions. These simulations will be used to confirm the accuracy of the simulation. Use calibration and background data to produce high stats data-sets using proposed new measurements of γ-ray flux, atmospheric neutron and muon backgrounds.

10.5.8 Task 8 : Develop reconstruction algorithms

a robust reconstruction will be developed for the data analysis. Recent methods based on template matching or multi-variate analysis will be investigated and benchmarked with the simulation.

10.5.9 Task 9 : Produce realistic unoscillated spectrum

The analysis will require realistic expectation of the anti-neutrino flux seen at various distances including the effect of the known backgrounds.

10.5.10 Milestones

Name	Definition	Date
WP4M1	Complete Simulation of reactor core	Jun 2014
WP4M2	Produce final detector geometry	Sep 2014
WP4M3	Produce realistic antineutrino flux calculation	Dec 2014
WP4M4	Tune detector response to data	Jan 2015
WP4M5	Freeze IBD selection and background reduction cuts	Feb 2015
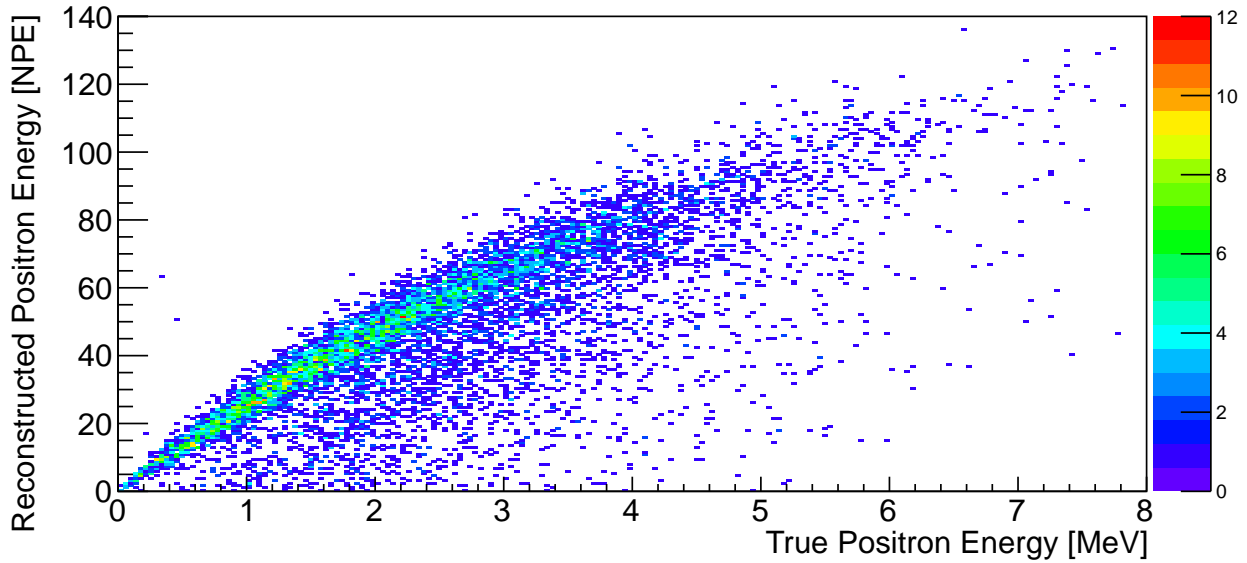
Figure 25: Reconstructed visible vs. true energy for positron interactions in the SoLi∂ detector. The observed non-linearity is due to the photon interaction process in the MPPC and can be easily corrected.

10.6 Resources requested

To achieve these goals we need the resources summarised in tables 10.

Table 10: WP4 manpower

Individual	Task	SY				PPRP
		Y1	Y2	Y3	total	
University of Oxford						
P. Scovell	Detector simulation	0.1	0.1	0.2	0.4	0.32
SubaTech						
M. Fallot	work package leader	0.1	0.1	0.1	0.3	0
L. Giot	reactor core simulation	0.1	0.1	0.1	0.3	0
WA	working allowance	0.03	0.03	0.03	0.1	0.08

10.7 Output

The deliverables of the work package are a reference anti-neutrino spectrum in a suitable format (MySQL tables for instance on a common repository), a simulation of the detector response to compare the expected neutrino rate and spectrum to data at various distances and a reconstruction of IBD events to perform the data analysis.

References

[1] K. Abe *et al.*,"Indication of electron neutrino appearance from an accelerator-produced off-axis muon neutrino beam", Phys. Rev. letters 107 (2011)

[2] P. Adamson *et al.*,"Improved search for Muon-neutrino to Electron-neutrino oscillation in MINOS", Phys. Rev. Letters 107 (2011)

[3] Indication for the disappearance of reactor electron antineutrinos in the Double Chooz experiment, Y. Abe et al. Phys. Rev. Lett. 108, 131801, (2012).

[4] Observation of electron-antineutrino disappearance at Daya Bay, Daya bay Collaboration, arXiv:1203.1669v2

[5] Observation of Reactor Electron Antineutrino Disappearance in the RENO Experiment, Reno Collaboration, arXiv:1204.0626

[6] F. Kaether, W. Hampel, G. Heusser, J. Kiko, and T. Kirsten, Phys.Lett. B685, 47 (2010), arXiv:1001.2731

[7] J.Abdurashitov *et al.* (SAGECollaboration), Phys.Rev.C80, 015807 (2009), arXiv:0901.2200.

[8] C. Giunti and M. Laveder, statistical Significance of the Gallium Anomaly, Phys.Rev. C83, 065504 (2011), arXiv:1006.3244

[9] T. A. Mueller et al. Improved Prediction of Reactor Antineutrino Spectra, Phys. Rev. C 83 (2011)

[10] G. Mention et al, The Reactor Antineutrino Anomaly, Phys. Rev. D 83 (2011)

[11] P. Huber,On the determination of reactor Antineutrino Spectra from nuclear reactors, Phys. Rev. C 84

[12] K. N. Abazajian *et al.*, "Light Sterile neutrino: a white paper", arXiv:1204.5379

[13] K. M. Heeger *et al.*, "Experimental parameters for a Reactor Antineutrino Experiment at very short Baeslines", arXiv:1212.2182

[14] A. Hahn, K. Schreckenbach, G.Colvin, B. Krusche, W. Gelletly*et al.*,

[15] See http://www2.physics.ox.ac.uk/research/mars-project

[16] A. Vacheret, G.J. Barker, M. Dziewiecki, et al. Characterization and simulation of the response of multipixel photon counters to low light levels. Nuclear Instruments and Methods in Physics Research Section A: Accelerators, Spectrometers, Detectors and Associated Equipment, 656(1):69-83, 2011.

[17] D. Yu. Akimov, H.M. Araujo, E.J. Barnes, V.A. Belov, A.A. Burenkov, et al. The ZEPLIN-III Anti- Coincidence Veto Detector. Astropart.Phys., 34:151-163, 2010.

[18] L. Reichhart, D. Yu. Akimov, H.M. Araujo, E.J. Barnes, V.A. Belov, et al. Quenching Factor for Low Energy Nuclear Recoils in a Plastic Scintillator. Phys.Rev., C85:065801, 2012.

A Annexe-1: Finance Tables

Summary of total costs		Cost £K			
		FY1	FY2	FY3 ...	Total
New Staff costs Including DI and DA staff and any staff costs under Exceptions	IMPERIAL	16.3	33.1	16.8	66.1
	OXFORD	26.0	56.6	17.0	99.6
	STFC Laboratory				
Equipment	DI and Exceptions				
Travel and Subsistence		8.8	45.7	2.9	57.4
Other costs	Other DI	332.4	268.7	0.0	601.2
	Other DA	1.3	2.7	1.0	4.9
	Exceptions				
Indirect Costs		44.4	94.2	33.7	172.2
Estate Costs		15.9	33.5	12.6	61.9
Working allowance		29.6	20.7	0.3	50.6
Contingency		0	151.0	100.0	251.0
Total "new costs" to STFC		474.6	706.2	184.1	1364.9
Existing Grant resources		82.7	130.9	36.1	249.6
Grand Total		1031.9	1543.2	404.3	1614.6

Figure 26: Overall cost to STFC

List individual items/groups of items	Institution		Cost			
			FY1	FY2	FY3	Total
New Staff Include DI and DA staff, laboratory staff, and any staff costs under exceptions (e.g. project students), itemised by staff member.						
Total New Staff						
Equipment *Where possible an itemised list should be provided which should be easy to cross-check with the justification of resources, split by institution.*						
Travel and subsistence	OXFORD		6,480	27,520	1,920	35,920
Split by institution.	ICL		2,320	18,160	960	21,440
Other costs		Other DI				
Itemised where possible; split out the DI, DA and Exceptions costs; split by institution.		Other DA				
		Exceptions				
Indirect Costs	HEI 1					
Split by institution.	HEI 2					
	etc.					
Estate Costs	HEI 1					
Split by institution.	HEI 2					
	etc.					
Working Allowance			836	4,340	274	5,449
Total Non-staff			9,636	50,020	3,154	62,809
Total 'new' cost			9,636	50,020	3,154	62,809
Existing grant resources	OXFORD	A. Vacheret (AF)	4,397	8,702	4,398	17,496
		A. Weber (CG)	4,247	9,557	2,124	15,928
	Imperial College London	J. Nash (CG)	1,266	2,317	2,210	5,793
Grand Total			19,547	70,595	11,884	102,027

Figure 27: WP1 cost table

List individual items/groups of items	Institution		Cost			
	Institution		FY1	FY2	FY3	Total
New Staff Include DI and DA staff, laboratory staff, and any staff costs under exceptions (e.g. project students), itemised by staff member.	Imperial College London	PDRA1 (DI)	16,257	33,052	16,798	66,107
	University of Oxford	Paul Scovel (DI)	13,163	30,068	10,173	53,405
	STFC Laboratory					
Total New Staff			29,420	63,120	26,971	119,511
Equipment *Where possible an itemised list should be provided which should be easy to cross-check with the justification of resources, split by institution.*						
Travel and subsistence *Split by institution.*						
Other costs	ICL	Other DI - Cons.	146,436	45,120	0	191,556
		Other DA	535	1,073	538	2,146
	OXFORD	Other DI - Cons.	97,624	30,080	0	127,704
		Other DI - Facil.	31,224	65,736	0	96,960
Itemised where possible; split out the DI, DA and Exceptions costs; split by institution.		Other DA	307	777	274	1,358
		Exceptions				
Indirect Costs	ICL		15,619	31,325	15,705	62,650
Split by institution.	OXFORD		12,099	30,580	10,776	53,455
Estate Costs	ICL		6,921	13,881	6,959	27,762
Split by institution.	OXFORD		3,775	9,541	3,362	16,677
Working Allowance			24,406	7,520	0	31,926
Total Non-staff			338,947	235,632	37,614	612,193
Total 'new' cost			368,367	298,752	64,585	731,705
Existing grant resources	ICL		27,860	48,666	0	76,526
Split by institution.	OXFORD	A. Vacheret (AF)	8,794	17,404	8,795	34,993
Grand Total			405,021	364,822	73,380	843,223

Figure 28: WP2 cost table

List individual items/groups of items			Cost			
	Institution		FY1	FY2	FY3	Total
New Staff Include DI and DA staff, laboratory staff, and any staff costs under exceptions (e.g. project students), itemised by staff member.	**OXFORD**	**Elec. Eng1**	**7,747**	**23,240**	**0**	**30,987**
		A. Baird	**1,795**	**0**	**0**	**1,795**
	STFC Laboratory					
Total New Staff			**9,542**	**23,240**	**0**	**32,782**
Equipment *Where possible an itemised list should be provided which should be easy to cross-check with the justification of resources, split by institution.*						
Travel and subsistence *Split by institution.*						
Other costs	**OXFORD**	Other DI - Cons.	44,000	88,400	0	132,400
		Other DI - Facil.	13,133	39,398	0	52,531
Itemised where possible; split out the DI, DA and Exceptions costs; split by institution.		Other DA	346	734	0	1,080
		Exceptions				
Indirect Costs	**OXFORD**		13,611	28,881	0	42,492
Split by institution.	ICL					
Estate Costs	**OXFORD**		4,247	9,011	0	13,257
Split by institution.	ICL					
Working Allowance			4,400	8,840	0	13,240
Total Non-staff			**79,737**	**175,264**	**0**	**255,001**
Total 'new' cost			**89,279**	**198,504**	**0**	**287,783**
Existing grant resources	ICL		7,598	9,270	13,257	30,125
Split by institution.	**OXFORD**		28,528	34,946	5,309	68,783
Grand Total			**125,405**	**242,720**	**18,567**	**386,691**

Figure 29: WP3 cost table

List individual items/groups of items			Cost			
	Institution		FY1	FY2	FY3 ...	Total
New Staff Include DI and DA staff, laboratory staff, and any staff costs under exceptions (e.g. project students), itemised by staff member.	OXFORD	P. Scovell (DI)	3,291	3,341	6,782	13,414
	STFC Laboratory					
Total New Staff			3,291	3,341	6,782	13,414
Equipment *Where possible an itemised list should be provided which should be easy to cross-check with the justification of resources, split by institution.*						
Travel and subsistence *Split by institution.*						
Other costs		Other DI				
Itemised where possible; split out the DI, DA and Exceptions costs; split by institution.	OXFORD	Other DA	77	86	183	346
		Exceptions				
Indirect Costs	**OXFORD**		3,025	3,398	7,184	13,606
Split by institution.	**HEI 2**					
	etc.					
Estate Costs	**OXFORD**		944	1,060	2,241	4,245
Split by institution.	**HEI 2**					
	etc.					
Working Allowance			0	0	0	0
Total Non-staff			4,045	4,544	9,608	18,197
Total 'new' cost			7,336	7,885	16,390	31,611
Existing grant resources *Split by institution.*						
Grand Total			7,336	7,885	16,390	31,611

Figure 30: WP4 cost table

Cost to STFC for University of Oxford

Institute: University of Oxford			FY1		FY2		FY3		TOTAL	
Staff Name	WP	Staff type	Cost (STFC)	FTE	Cost (STFC)	FTE	Cost (STFC)	FTE	Cost (STFC)	FTE
A. Vacheret	1	STFC Adv. Fellow		0.1		0.2		0.1		0.4
A. Vacheret	2	STFC Adv. Fellow		0.2		0.4		0.2		0.8
A. Weber	1	CG - Physicist		0.04		0.09		0.02		0.15
A. Weber	3	CG - Physicist		0.15		0.25		0.05		0.45
A. Baird	3	CG- Engineer		0.15		0.1		0		0.25
Total CG and other posts				**0.64**		**1.04**		**0.37**		**2.05**
Paul Scovell	2	DI - PDRA	13,163	0.4	30,068	0.9	10,173	0.3	53,405	1.6
Paul Scovell	4	DI - PDRA	3,291	0.1	3,341	0.1	6,782	0.2	13,414	0.4
Elec. Eng1	3	DI - Elec. Eng	7,747	0.25	23,240	0.75	0	0	30,987	1
A. Baird	3	DI - Elec. Eng	1,795	0.05	0	0	0	0	1,795	0.05
Total new posts			**25,996**	**0.8**	**56,650**	**1.75**	**16,956**	**0.5**	**99,601**	**3.05**
DI costs										
Travel and Subsistence			6,480		27,520		1,920		35,920	
Other DI Consumables - WP2			97,624		30,080		0		127,704	
Other DI Consumables - WP3			44,000		88,400		0		132,400	
Other DI Facilities - Mech. Design SRF			7,320		0		0		7,320	
Other DI Facilities - Mech. w/s SRF			23,904		65,736		0		89,640	
Other DI Facilities - Elec. tech. w/s SRF			13,133		39,398		0		52,531	
DA costs										
Estate costs (best estimate)			8,965		19,611		5,603		34,180	
Other DA – Infrastructure technician			730		1,597		456		2,784	
Indirect costs (best estimate)			28,735		62,859		17,960		109,554	
Total 'new' costs			256,887		391,851		42,895		691,633	
excl. CG costs										
Total Consolidated Grant resource			32,775		44,503		7,433		84,710	
Total other STFC grant			13,191		26,106		13,193		52,489	
Grand total			302,853		462,459		63,520		828,833	
incl. CG & other STFC grant costs										

Figure 31: Cost per institute University of Oxford

Cost to STFC for Imperial College London

Institute: Imperial College London			FY1		FY2		FY3		TOTAL	
Staff Name	WP	Staff type	Cost (STFC)	FTE	Cost (STFC)	FTE	Cost (STFC)	FTE	Cost (STFC)	FTE
J. Nash	1	CG - Physicist		0.025		0.05		0.025		0.1
G. Barber	2	CG - Engineer		0.25		0.33		0		0.58
A. Rose	3	CG - Engineer		0.15		0.2		0.15		0.5
M. Khaleeq	2	Other - Technician		0.1		0.24		0		0.34
V. Casey	2	CG - Technician		0.1		0.24		0		0.34
Mech. Tech.	2	CG - Technician		0.1		0.24		0		0.34
Total CG and other posts				**0.725**		**1.3**		**0.175**		**2.2**
PDRA1	2	DI - PDRA	16,257	0.5	33,052	1	16,798	0.5	66,107	2
Total new posts			**16,257**	**0.5**	**33,052**	**1**	**16,798**	**0.5**	**66,107**	**2**
DI costs										
Travel and Subsistence - WP2			2,320		18,160		960		21,440	
Other DI Consumables - WP2			146,436		45,120		0		191,556	
DA costs										
Estate costs (best estimate)			6,921		13,881		6,959		27,762	
Other DA - Infrastructure technician			535		1,073		538		2,146	
Indirect costs (best estimate)			15,619		31,325		15,705		62,650	
Total 'new' costs			188,089		142,611		40,960		371,660	
excl. CG costs										
Total Consolidated Grant resource			36,725		60,253		15,467		112,445	
Grand total			224,814		202,863		56,427		484,104	
incl. CG costs										

Figure 32: Cost per institute Imperial College London

B Annexe-2: Risk Register

RiskRegisterSoLid-AV
29/04/2013

RISK REGISTER

Project Title:	soLid
Project Manager:	Vacheret
Last Update:	25-Apr-13

Total risk is product of Likelihood and impact
0 - 25	low
25 - 50	medium
50 - 100	high

Ref.	Risk Description	Potential impact on project	Owner	Inherent Risk			Existing Controls	Current/Proposed mitigation	Residual Risk			Risk Exposure		Action Required
				Likelihood	Impact	Total			Likelihood	Impact	Total	description	Cost (£k)	
WP1R1	Loss of key personnel	lack of leadership, delays to project	vacheret	0.1	100	10	keep good communication, Provide long term career planning	good communication, shared leadership	0.1	50	5			
WP1R2	inconsistencies between work in different WP	delay to project	vacheret	0.2	30	6	regular management meetings	design reviews and regular meetings with all stakeholders	0.1	30	3			
WP1R3	delays in funding	delays to project	vacheret	0.5	80	40	write proposal	write good proposal and respond speedily to comments	0.3	80	24			
WP1R4	Overspend on travel budget	inability to finish project	vacheret	0.1	50	5	monitor travel spending and control approval of travel	re-schedule work with fewer trips, draw on WA and contingency	0.1	20	2			
WP2R1	loss of key personnel	delay to project	vacheret	0.1	50	5	rely on permanent staff		0.1	50	5			
WP2R2	delay in sub-module design	general construction delay	buhour	0.2	30	6	management meetings	Barber will follow closely progress of design	0.2	30	6			
WP2R3	delay in module design	general construction delay	barber	0.2	40	8	management meetings	regular meeting with package manager	0.2	40	8	Engineer at Oxford/Subatech	15	draw on contingency
WP2R4	increased cost in module construction	smaller detector mass or draw on contingency	vacheret	0.2	80	16	design review	simplify design	0.1	40	4			
WP2R5	module constructions more complicated	delays and increased cost	vacheret	0.3	80	24	design review	simplify design	0.1	60	6			
WP2R6	electronics not available in-time	delays in commissioning detector	weber	0.2	50	10	management meetings	try to find additional manpower in WP3	0.1	50	5			
WP2R7	installation site not available	no experiment	vacheret	0.3	100	30	discussion with reactor sites	agree detector location and collaboration	0.1	100	10			
WP3R1	Loss of key personnel	delays to have working electronics	weber	0.1	40	4	contact with personnel, spread of knowledge		0.1	20	2	additional time needed to get person up to speed	10	
WP3R2	not being able to produce 64ch DPC	increased cost	weber	0.3	70	21	review firmware design and requirements	consider moving to larger FPGA	0.1	70	7	cost of additional DPC	70	may need bridging funding to de-risk development
WP3R3	delays in firmware development	delays to project or reduced capability	weber	0.3	30	9	review of firmware design	add additional manpower, if required	0.3	20	6	cost of additional E.Eng	50	
WP3R4	insufficient DAQ	need for more DAQ hardware	weber	0.2	80	16	move to more detailed DAQ design	move to full DAQ design	0.1	20	2	additional DAQ hardware	10	move to detailed DAQ design
WP4R1	Loss of key personnel	delay to project	fallot	0.3	30	9	spread knowledge among collaborators		0.3	30	9			
WP4R2	delay in delivering reactor flux	delay in analysis of data	fallot	0.1	20	2	regular meetings to review progress		0.1	20	2			
WP4R3	delay in delivering reconstruction	late changes to firmware implementation	fallot	0.1	30	3	try to finish basic neutron ID first		0.1	30	3			
						0					0			

Notes
Likelihood scale of 0.1 to 1 where 0.1 is low.
Impact scale of 1-100 where 1 is low.